The safety and efficacy of magnesium membrane with polymer-coating for guided bone regeneration in a rabbit calvarium model

토끼 두개골 모델에서의 중합체 코팅 마그네슘 차폐막의 골 유도 재생술에 대한 안전성 및 효용성

2023년 2월

서울대학교 대학원
치의과학과 구강악안면외과학전공

온 성 운

The safety and efficacy of magnesium membrane with polymer-coating for guided bone regeneration in a rabbit calvarium model

지도교수 최진영

이 논문을 치의과학박사 학위논문으로 제출함

2022년 11월

서울대학교 대학원
치의과학과 구강악안면외과학 전공

온 성 운

온성운의 박사학위논문을 인준함
2023년 1월

위 원 장   _____(인)
부위원장   _____(인)
위   원   _____(인)
위   원   _____(인)
위   원   _____(인)

Abstract

The safety and efficacy of magnesium membrane with polymer−coating for guided bone regeneration in a rabbit calvarium model

Sung−Woon On, D.D.S., M.S.D.

Program in Oral and Maxillofacial Surgery, Department of Dental Science, Graduate School, Seoul National University
(Directed by Professor **Jin−Young Choi**, D.D.S., M.D., Ph.D.)

Background and purpose: Guided bone regeneration (GBR) for implant placement is a predictive procedure. For space maintenance and stabilization of the graft material, non−resorbable barrier membranes such as expanded polytetrafluorethylene (e−PTFE), titanium−reinforced e−PTFE and titanium mesh are used. One of major drawbacks of using non−resorbable membranes including titanium mesh is that a secondary operation for removal is required. Therefore, a demand for a new barrier membrane has emerged. Magnesium (Mg) not only has the mechanical strength of metal but also is capable of biodegradation. During biodegradation, however, Mg alloys undergo rapid corrosion resulting in excessive hydrogen gas formation and premature loss of mechanical strength. There have been attempts to apply resorbable polymers including poly−L−lactic acid (PLLA) as surface treatment materials to prevent early

i

corrosion of Mg. However, most of them are *in vitro*-level studies and only a handful of *in vivo* studies have been published. There is a demand for more *in vivo* studies on the improved corrosion resistance of PLLA-coated Mg alloy and its safety and effectiveness. The aims of this study were to evaluate the safety and efficacy of PLLA-coated Mg membrane in GBR through *in vitro* and *in vivo* tests using a rabbit calvarium model.

Materials and methods: Uncoated Mg membrane and PLLA-coated Mg membranes were fabricated using a Mg-Dysprosium (Dy) alloy. With a scanning electron microscope (SEM), the microstructure of Mg membrane surface with or without PLLA-coating were examined and thickness of PLLA coating was measured. The *in vitro* degradation test was performed by immersing the Mg membranes into Dulbecco's modified Eagle medium (DMEM) and measuring the weight loss over immersion time. The *in vitro* cytotoxicity test was conducted according to ISO 10993-5, and 3-(4,5-dimethylthiazol-2-yl)-2,5-diphenyltetrazolium bromide (MTT) assay was performed. *In vivo* study was conducted using twenty-four healthy New Zealand white male rabbits. Two symmetrical 8 mm-diameter bone defects on each side of the rabbit calvaria were created using a trephine bur. In a total of 48 defects, 12 defects were randomly assigned per group according to the following four categories: (1) Negative control (NC) group: unfilled and left uncovered, (2) Positive control (PC) group: filled with graft material and left uncovered, (3) Uncoated Mg group: filled with graft material and covered with uncoated Mg membrane, (4) PLLA-coated Mg group: filled with graft material and covered with PLLA-coated Mg membrane. Xenogenic bone graft material (Bio-Oss®; Geistlich Pharma AG, Wolhusen,

Switzerland) was used to fill the defect. Clinical observation was conducted regularly, and eight rabbits (16 defects) were sacrificed at 4, 8, and 12 weeks to analyze the healing patterns for each study period. Radiological study using micro-computed tomography (micro-CT) and histological, histomorphometric, and immunohistochemical analyses were performed on each specimen. Statistical analyses were carried out to compare the differences in variables among the groups at each study period, and p values of less than 0.05 were considered statistically significant.

Results: The PLLA-coated Mg membrane showed smoother surface in general compared to the uncoated Mg membrane. The thickness of the PLLA coating was measured to be 9.91 ± 2.75 μm under SEM. The degree of degradation of uncoated Mg membrane and PLLA-coated Mg membrane indicated a favorable protective effect of PLLA coating. In cytotoxicity test, no deformed or degenerated cells based on qualitative morphological grading of cytotoxicity of extracts in ISO 10993-5 were observed in the samples from both uncoated Mg and PLLA-coated Mg membranes. The results of L-929 cell viability in MTT assay showed uncoated Mg membrane cell viability of 96.5% and PLLA-coated Mg membrane cell viability of 72%. According to the evaluation criteria of the MTT cytotoxicity test of ISO 10993-5, both membranes were confirmed to have no cytotoxic potential. In the *in vivo* study, no rabbits were lost during the experiment. During clinical observation, all rabbits, except for one, were healed without any complications. Radiological analysis using Micro-CT showed the PLLA-coated Mg group resulted in significantly higher percentages of new bone volume (NBV) and total bone volume (TBV) than the NC group at 4, 8, and 12 weeks (all $P < 0.05$). The residual membrane

surface area of the PLLA-coated Mg group was significantly higher than that of the uncoated Mg group at 4 weeks ($P < 0.05$). Upon histological observation, the PLLA-coated Mg group showed a large void area below the membrane, but the void was smaller and appeared later compared to the uncoated Mg group. PLLA-coated Mg group also showed more complete restoration of the bony contour than the uncoated Mg group. In terms of histomorphometric analysis, the PLLA-coated Mg group showed the highest percentage of total bone area (TBA) among all groups at all study periods and residual material area (RMA) at 8 and 12 weeks, but the differences were not statistically significant. Comparison of inflammatory response scores and the numbers of multinucleated giant cells (MNGCs) among the groups indicated that the PLLA-coated Mg group did not show significant differences from the NC and PC groups in inflammatory response scores and the numbers of MNGCs. In immunohistochemical analysis using osteocalcin (OC) and osteopontin (OPN), the percentage of OC expression in the PLLA-coated Mg group was significantly higher than that of the NC group at 8 weeks ($P < 0.05$), and the percentage of OPN expression in the PLLA-coated Mg group was significantly higher than that of the NC group at 4, 8, and 12 weeks (all $P < 0.05$).

Conclusions: Regarding the safety of PLLA-coated Mg membrane, PLLA-coated Mg membrane showed no cytotoxic effect according to *in vitro* cytotoxicity tests and demonstrated favorable biocompatibility as it did not cause significant inflammatory response histologically or clinically in an *in vivo* test using a rabbit calvarium model. In terms of efficacy, a slower degradation of PLLA-coated Mg membrane was observed than the uncoated Mg membrane in

iv

degradation test and micro-CT analysis. In addition, Mg membrane with PLLA coating showed good bone formation and maintenance in radiological and histomorphometric analyses. The results of this study indicates that PLLA-coated Mg membrane is a safe and effective material for GBR at both *in vitro* and *in vivo* levels.

CONTENTS

Introduction

   Guided bone regeneration (GBR) for dental implant placement is a fairly common procedure with high success rate, and it has been established through decades of research and clinical practice.[1] GBR enables dental implant placement in areas of bone loss by restoring the height and width of alveolar bone. Alveolar ridge augmentation procedure can be classified into horizontal ridge augmentation that restores the width of alveolar bone and vertical ridge augmentation that restores the height of alveolar bone. Between the two, the vertical ridge augmentation is considered more technically demanding and less predictable than horizontal ridge augmentation.[2] Among many requirements for a successful GBR,[3] the factors related to the success of vertical ridge augmentation include space maintenance, stability of the graft material, and primary wound closure that withstands the tension of soft tissue. For better space maintenance and stabilization of the graft material, non−resorbable barrier membranes such as expanded polytetrafluorethylene (e−PTFE), titanium−reinforced e−PTFE and titanium mesh are often used for vertical ridge augmentation. Titanium mesh is the only commercially available barrier membrane made of metal. It has excellent biocompatibility and mechanical support, fulfilling the

requirements for a successful vertical bone augmentation.[4] In spite of these advantages, non-resorbable membranes including titanium mesh have a major drawback which is the need for a secondary operation for removal. Membranes made of resorbable materials such as collagen lack rigidity, making space maintenance difficult under soft tissue tension. As a result, the use of the resorbable membrane is limited in vertical alveolar bone augmentation. Therefore, there has been a rising demand for the development of a resorbable metal barrier membranes with mechanical stability comparable to titanium mesh.

Magnesium (Mg) is a resorbable material with the mechanical strength of metals. Mg alloys had been tested for application in the fields of orthopedic and vascular surgery in as early as the late 1800s.[5] However, they have lost interest due to the characteristic rapid corrosion resulting in the formation of excessive hydrogen gas and premature loss of mechanical strength. Recently, however, a number of studies on the prevention of rapid corrosion of Mg have been conducted, and Mg has been regaining attention. In applications for Mg alloys, rare earth elements are known to play an important role in enhancing the corrosion resistance by removing impurities of Mg alloy and purifying the matrix.[6] In consideration of this point, studies have been carried out to examine the biological performance

of Mg alloys containing rare earth elements as resorbable implants.[7,8] However, Mg alloy containing rare earth elements has been mainly used in research for drug eluting stents or plate and screw for bone fixation, and has not been used for fabrication of membrane in GBR. In the last 5 years, several studies have been conducted reporting that these alloys showed good biocompatibility and mechanical strength when used for fixation plates, screws, and implants in the craniomaxillofacial area,[9-11] and based on these studies, expectations for application of Mg alloys containing rare earth elements as barrier membranes have risen. Resoloy® (MeKo, Hannover, Germany) is a Mg alloy containing rare earth elements based on Mg−Dysprosium (Dy), and was developed for resorbable implants. Dy, which has high solubility in Mg, and can be combined with other elements such as zirconium (Zr), neodymium (Nd), and gadolinium (Gd) to control the mechanical and corrosion properties, and Mg−Dy alloy demonstrated good cytocompatibility *in vitro*.[12,13] In addition, Resoloy® showed excellent corrosion behavior and mechanical properties including strength and ductility with an optimized microstructure in previous report.[14] Therefore, it is necessary to try using Resoloy® as a basic material for the membrane in GBR.

Among various methods to increase the corrosion resistance and biocompatibility of Mg, alloying or surface treatment such as coating

technique are mainly applied.[15,16] Surface coating technique is a method of forming a lining layer of different composition to keep Mg from contacting with corrosive fluids. The coating method is considered more convenient and timesaving compared to the alloying technique.[17] The surface coating technique is classified into the following two methods according to the participation of substrates: conversion coating and deposited coating. Between the two, the deposited coating is formed *ex situ* without the substrate participation, and the composition of coating is more flexible than the conversion coating.[18,19] Both organic and inorganic materials are used as protective physical coating, but organic materials such as resorbable polymers are preferred for their superior protective function and minimal spatial defects.[20] In addition, polymeric coating, which occupies the majority of deposited coatings, is expected to show excellent corrosion resistance and bioactive performance in Mg−based materials because it can be easily tailored and can act as a carrier for bioactive compounds.[21,22] Therefore, attempts to improve both the corrosion resistance and biocompatibility of Mg alloy using such resorbable polymers are ongoing.

The resorbable synthetic polymers include polyglycolic acid (PGA), polylactic acid (PLA), poly(lactic−*co*−glycolic) acid (PLGA). These polymers are biocompatible and slowly degraded, allowing for clinical

application in various fields that meet the purpose. By focusing on the characteristics of these resorbable polymers, there have been attempts to apply the resorbable polymers as surface treatment materials to prevent early corrosion of Mg.[23-27] These studies have shown the possibility of better corrosion resistance of Mg, but most of them are *in vitro*-level studies, and only a handful of *in vivo* studies have been published. In particular, there are no *in vivo* studies on poly-L-lactic acid (PLLA) as a surface coating for Mg membrane used for GBR. PLLA is known to have a longer degradation period than the other type of PLA, poly-D-lactic acid (PDLA).[28,29] It is of both academic and clinical interest to examine the corrosion resistance of PLLA-coated Mg alloy by *in vivo* test, and evaluate its safety and effectiveness.

Therefore, the aims of the present study were to evaluate the biocompatibility and safety of PLLA-coated Mg membrane, and to investigate the efficacy of PLLA-coated Mg membrane in GBR.

Materials and methods

A. *In vitro* study

1. Preparation of PLLA-coated Mg membrane

The uncoated Mg membrane and PLLA-coated Mg membrane used

in the present study were fabricated at MeKo Manufacturing e.K. (Hannover, Germany) from Resoloy®, a Mg−Dy−Nd−zinc (Zn)−Zr alloy. Initially, a mesh type cylindrical Mg tube with a diameter of 8 mm as shown in Figure 1 was cut in half to become a hemispherical shape, and then further cut to have a length of 12 mm by laser (high end laser systems developed and built by MeKo) cutting with tolerances of ±0.005 mm. Then, the hemispherical Mg tube was flattened as much as possible by folding the middle part using a bending jig (Figure 2). As a result, Mg membranes with dimensions of 11.5 mm × 12.0 mm × 0.7 mm were completed, and had a thickness of 0.2 mm and a weight of 32.6 mg. Prior to PLLA coating, cleaning with ethanol was performed as a pretreatment process. PLLA coating was carried out through common spray coating using a company−specific process. Each uncoated Mg membrane and PLLA− coated Mg membrane were sterilized with ethylene oxide (EO) gas before *in vitro* and *in vivo* tests.

2. Microstructure of Mg membrane with or without coating

The microstructure of surface of Mg membrane with or without PLLA−coating were observed using scanning electron microscope (SEM) (Gemini SEM 300; Carl Zeiss, Jena, Germany). SEM samples were analyzed after platinum coating. The measurement of thickness

of PLLA coating was also performed using SEM.

3. Degradation test

The *in vitro* degradation test was performed by immersing the Mg membranes with or without coating into Dulbecco's modified Eagle medium (DMEM; Welgene, Gyeongsan, Republic of Korea) and measuring the weight loss over immersion time. Before immersion, the initial weight (W_0) of each uncoated Mg membrane and PLLA-coated Mg membrane was measured. After EO sterilization, each membrane was immersed in 2 mL of DMEM medium containing 10% fetal bovine serum (FBS) (Hyclone, Logan, USA), 1% Penicillin-Streptomycin (Gibco, Waltham, USA) and 5M NaCl (Samchun Pure Chemical Co., Pyeongtaek, Republic of Korea). Samples were immersed for 50 days, and the medium was replaced every 48 hours. Three samples for each uncoated Mg membrane and PLLA-coated Mg membrane were taken out, washed, dried and weighed (W_1) at 5-day intervals. The weight loss was calculated as follows:

Weight loss = (W_0 − W_1)/ W_0 X 100%

In addition, photographic images were taken to investigate the change in the shape of the membranes according to the weight change

during the degradation test. Confirmation of shape change was performed at the initial (day 5), middle (day 20), and end (day 50) points of the test.

4. Cytotoxicity test

The *in vitro* cytotoxicity test was conducted according to ISO 10993-5. The test was performed by the direct contact method, and the samples were sterilized through EO sterilization before use. L-929 cells were cultured using RPMI 1640 media (Hyclone, Logan, USA) containing 10% FBS and 1% Penicillin-Streptomycin, and incubated at 37℃ under the condition of 5% CO_2 for 24 hours. One day before the start of the experiment, 2×10^6 cells in 2000 uL were seeded in each well of 6-well plates and subcultured for 24 hours. After that, when the cell density per well reached 70%, sample (uncoated Mg membrane and PLLA-coated Mg membrane), positive control (PC) [a medium containing 10% FBS and 10% dimethyl sulfoxide (DMSO; Sigma-Aldrich, St. Louis, USA)], and media control (MC) (a medium containing 10% FBS) were added and cultured for 24 hours. Then, the growth inhibition and lysis state of the cells were observed under an inverted light microscope (Nikon Eclipse TS100; Nikon, Tokyo, Japan) and microscopic images were taken. After removing the existing medium, 2 ml of 3-(4,5-

dimethylthiazol-2-yl)-2,5-diphenyltetrazolium bromide (MTT) solution (Sigma-Aldrich, St. Louis, USA) and RPMI medium at a ratio of 1:9 were dispensed into each well, and incubated for 3 hours at 37℃ and 5% CO_2 incubator. After removing the MTT solution, DMSO was treated, and the cells were removed from the surface of plate and put into a microplate reader (PowerWave XS2; BioTek instruments Inc., Winooski, USA) to measure absorbance, thereby performing MTT assay.

B. *In vivo* study

1. Experimental animals

The *in vivo* study was performed in a contract research facility (Cronex Co., Ltd., Hwaseong, Republic of Korea) using twenty-four healthy New Zealand white male rabbits (weight 2.5 - 3.0 kg). The animals were housed in individual cages under standard laboratory conditions, and were fed a regular dry diet and water ad libitum. All animals had an acclimatization period of 2 weeks prior to the experiments. The protocol for this experiment was reviewed and approved by the Institutional Animal Care and Use Committee (IACUC) of the testing facility (CRONEX-IACUC: 202202005). Eight rabbits (16 defects) were randomly assigned at each time point of the study (4, 8 and 12 weeks).

2. Surgical procedure

The rabbits were anesthetized by intramuscular injection of zoletil (15mg/kg; VIRBAC S.A., Carros, France) and xylazine (5mg/kg; Bayer Korea Co., Ansan, Republic of Korea). Before surgery, the rabbits' hair was shaved, and the surgical site was disinfected with betadine and then draped. A 5 cm midsagittal full-thickness incision was performed from the frontal bone to the occipital bone. The flaps were reflected bilaterally to expose the entire skull. After flaps including the skin and periosteum were properly retracted, two bone defects symmetrical to the midline of the calvaria with a diameter of 8 mm were created carefully using a trephine bur (Hager & Meisinger GmbH, Neuss, Germany). A total of 48 defects generated in 24 rabbits were randomly assigned to the following four groups: unfilled and left uncovered without membrane for the negative control group (NC group, 12 defects), filled with graft material and left uncovered for the positive control group (PC group, 12 defects), filled with graft material and covered with uncoated Mg membrane for the uncoated Mg group (12 defects), and filled with graft material and covered with PLLA-coated Mg membrane for the PLLA-coated Mg group (12 defects) (Figure 3). In order to minimize the change in results due to the graft material, only Bio-Oss® (Geistlich Pharma AG, Wolhusen,

Switzerland), which shows efficacy, stability, and high success rate in GBR procedures,[30-32] was used as the bone graft material. Regarding membranes, in order to adhere to the bone surface as much as possible and to facilitate primary sutures, the central part was pressed and flattened in the existing design form as shown in Figure 2. The distance between the edge of the membranes and the margins of the defects was at least 1.5 mm. The periosteum was tightly sutured using 4-0 Vicryl (Ethicon, Somerville, USA) to secure the membrane, and the skin was sutured using 4-0 Nylon (Ailee Co., Busan, Republic of Korea). After surgery, antibiotics (enrofloxacine, 4 mg/kg) and analgesics (meloxicam, 0.4 mg/kg) were applied intramuscularly for 3 days. All rabbits recovered after surgery without any complications. At each time point, rabbits were euthanized by intramuscular injection of succipharm (25 mg/kg; Komipharm Co., Siheung, Republic of Korea) after inducing preanesthesia by intramuscular injection of 0.1 ml/kg of a 1:1 mixed solution of zoletil and xylazine. After sacrifice of the experimental animals, calvarial bones including the surgical sites were carefully excised and harvested.

3. Clinical observations

   All rabbits were observed daily until euthanasia to evaluate

inflammatory signs and complications at the surgical site. If signs such as wound dehiscence, membrane exposure, edema, or fistula formation were observed, they were checked and recorded weekly. Such signs were evaluated closely by comparing photographs.

4. Micro-computed tomography (micro-CT) analysis

For quantitative measurement of the bone changes in the healing sites of calvarial bones and the residual amounts of Mg membranes, micro-CT (SkyScan1173; Bruker, Kontich, Belgium) scans were performed on the specimens of each group at each time period. As scan conditions, the tube voltage and current were 130 kVp and 60 μA, respectively, and 1 mm aluminum filter was used. The exposure time was 500 ms, and a rotation angle of 0.3 degree was applied. A total of 800 images with 2240 $\times$ 2240 pixels and a pixel size of 25 μm were obtained. Nrecon (Bruker, Kontich, Belgium) was used for cross-sectional reconstruction, and Data Viewer (Bruker, Kontich, Belgium) and Ct-VOX (Bruker, Kontich, Belgium) were utilized for three-dimensional (3D) reconstruction. An 8 mm diameter cylindrical healing area was set as the region of interest (ROI), and the height was set by designating the line connecting the upper edge of the margins on both sides of the defect as the top and the line connecting the lower edge as the bottom. Specific grayscale

thresholds were set to distinguish the newly formed bone, graft material, and soft tissue, and quantitative analysis of tissues was performed by setting the total bone area to a range of level 58−255, newly−formed bone to level 58−89, and graft material to level 90−255, respectively. For measurement of the volume and surface area of the residual Mg membrane, the area of each residual membrane was set and analyzed using the cross−sectional image in 3D reconstruction. The parameters in the micro−CT analysis were as follows.

- Percentage of new bone volume (NBV): percentage of new bone volume to total tissue volume within the ROI.
- Percentage of residual material volume (RMV): percentage of residual graft material volume to total tissue volume with the ROI.
- Percentage of total bone volume (TBV): percentage of sum of NBV and RMV to total tissue volume within the ROI.
- Residual volume (mm^3) of membrane: the volume of the remaining membrane above the defect.
- Residual surface area (mm^2) of membrane: the surface area of the remaining membrane above the defect.

5. Histological and immunohistochemical processing

After the micro-CT analysis, harvested samples were processed for histological and immunohistochemical analyses. After fixing each tissue specimen in buffered neutral formalin (Sigma-Aldrich Co. LLC., St. Louis, USA) solution for 1 week, the tissue specimen was decalcified with 10% EDTA solution for 3 weeks, dehydrated while increasing the concentration of ethanol, and embedded in paraffin. The embedded tissue block was cut into $3-\mu$m-thick sections using a microtome (Leica RM2255 rotary microtome; Leica Microsystems, Buffalo Grove, USA), and stained with hematoxyline and eosin (H & E) or Masson-Goldner trichrome (MT) to evaluate formation of new bone, residual graft material, and total bone area.

For further evaluation of bone remodeling and mineralization, immunohistochemistry was performed to detect the expression of osteocalcin (OC) and osteopontin (OPN). The sectioned tissue slides were deparaffinized, hydrated, washed, and stained using anti-OC (clone OC4-30; dilution 1:100; Invitrogen, Waltham, USA) and anti-OPN (clone 1B20; dilution 1:100; Novus Biologicals, Cambridge, UK) as primary antibodies. After dispensing EnVision™+ Horse Radish Peroxidase (HRP) (Dako Corporation, Hamburg, Germany) as a secondary antibody, the reaction was performed at room temperature for 1 hour, followed by washing with phosphate buffered saline (PBS)

3 times for 5 minutes. Then, the slices were applied with diaminobenzidine (DAB) as a chromogen for 1 min, washed with PBS, and counterstained with Mayer's hematoxylin.

All stained tissue slides were digitally imaged using a digital slide scanner (Pannoramic 250 Flash III; 3DHISTECH, Budapest, Hungary) and then observed using a viewer program (CaseViewer version 2.4; 3DHISTECH, Budapest, Hungary).

6. Histological, histomorphometric, and immunohistochemical analyses

All histological, histomorphometric, and immunohistochemical analyses were performed by a single investigator who was blinded to the group assignment. The ROIs for all histological analyses except for the evaluation of inflammatory response were defined identically to the ROIs established in the micro-CT analysis. For quantitative evaluation of healed defects, the percentages of newly formed bone, residual graft material, and total bone mass was measured using Image-Pro Plus (Media Cybernetics, Rockville, USA), and calculated using the following formulae.

- Percentage of new bone area (NBA) (%): percentage of new bone area to total tissue area.

- Percentage of residual material area (RMA) (%):

  percentage of residual material area to total tissue area.

- Percentage of total bone area (TBA) (%): percentage of

  sum of NBA and RMA to total tissue area.

In terms of examining the *in vivo* safety of Mg membrane with or without coating, the inflammatory response was evaluated. The inflammatory response scoring system with a scale of 0-5 was applied to grade the degree of inflammatory response of each section, and the scale was graded by setting 0 as negative of inflammatory cells, 1 as the minimal number of inflammatory cells, and 5 as the very large number of inflammatory cells, comparatively evaluating the degree of inflammation (Figure 4). Additionally, the number of multinucleated giant cells (MNGCs) observed in the specimens was evaluated, and the number of MNGCs observed at x400 magnification on the H & E-stained specimens was analyzed. Evaluation of Inflammatory response and measurement of number of MNGCs were performed by setting the entire defect as an ROI, including the membrane-existing area above the defect.

In order to evaluate the expression level of immunohistochemical staining of OC and OPN in each specimen, the area of the immunopositive area to the entire ROI was measured as a percentage

using the same program (Image-Pro Plus) applied for histomorphometric analysis.

7. Statistical analysis

The mean and standard deviation of the data were expressed in graphs. For evaluation of the normality of the data, the Shapiro-Wilk test were used. Kruskal-Wallis test was used to compare the differences in variables among the groups at each study period, and Mann-Whitney test with Bonferroni correction was applied as a post hoc test. For comparison of residual volume and surface area of Mg membrane between the uncoated and PLLA-coated Mg group, independent t-test was performed. P values of less than 0.05 were considered statistically significant. All statistical analyses were performed using SPSS 21.0 (SPSS Inc, Chicago, USA).

Results

A. *In vitro* study

1. Microstructure of uncoated Mg membrane and PLLA-coated Mg membrane

   The SEM images of the uncoated Mg membrane and PLLA-coated Mg membrane are presented in Figure 5 and Figure 6, respectively.

In the image at x10 magnification, the PLLA－coated Mg membrane showed an overall smoother surface than the uncoated Mg membrane, and in the images at x50 and x100 magnification, the pores that were present in the uncoated Mg membrane were not observed in the coated Mg membrane. In addition, defects such as shell cracking, finning, and metal penetration on the surface of coated Mg membrane were not observed in the images at x300 and x500 magnifications. The thickness of the PLLA coating was measured to be 9.91 ± 2.75 μm by SEM (Figure 7).

2. *In vitro* degradation of coated and uncoated Mg membrane

The results of observing the degradation degree of uncoated Mg membrane and PLLA－coated Mg membrane in DMEM medium according to weight change are presented in Figure 8. In the case of the uncoated Mg membrane at the beginning of the degradation test, a change in weight was observed to some extent, but in the case of the PLLA－coated Mg membrane, no significant change in weight was observed until the 20th day. Both membranes showed a significant change in weight from the 20th to the 30th day, and the weight steadily decreased from the 30th day to the end of the test. The weight loss up to the 50th day, the end point, was about 25% for uncoated Mg membrane and about 11% for PLLA－coated Mg

membrane, indicating a favorable protective effect of PLLA coating.

Photographic images of the change in the shape of the membrane according to the weight change during the degradation test are shown in Figure 9. On the 5th day of the test, no structural change was observed in uncoated Mg membrane, but overall degradation was observed on the surface of the membrane. However, PLLA-coated membrane appeared to be partially degraded. On the 20th day of the test, both membranes were highly degraded, and in particular, the breakage of mesh lattice in the uncoated Mg membrane was observed. On the 50th day, more than half of the lattice of the uncoated Mg membrane was broken, and the partial breakage of lattice of the PLLA-coated Mg membrane was also observed, but it showed a similar degree to that of the uncoated Mg membrane on the 20th day.

3. *In vitro* cytotoxicity of coated and uncoated Mg membrane

Microscopic observation of the growth inhibition and lysis state of L-929 cells after treatment with samples, MC, and PC are presented in Figure 10. As a result of evaluating the cytotoxicity based on qualitative morphological grading of cytotoxicity of extracts in ISO 10993-5 by observing the number and shape of the cells, no deformed or degenerated cells were observed in the samples of uncoated Mg and PLLA-coated MG membranes (Table 1).

The results of L-929 cell viability in MTT assay are shown in Figure 11. The uncoated Mg membrane showed cell viability of 96.5%, whereas the PLLA-coated Mg membrane showed cell viability of 72%, which is slightly lower than that of uncoated Mg membrane. However, based on the evaluation criteria of the MTT cytotoxicity test of ISO 10993-5, both membranes were confirmed to have no cytotoxic potential.

B. *In vivo* study

1. Clinical observations

No rabbits in the present study were lost during the experiment. All rabbits, except for one, were healed without any complications such as wound dehiscence, membrane exposure, edema, or fistula formation. In one case, swelling at the surgical site was observed from the 1st to 2nd weeks after the operation, but it resolved spontaneously and showed no special signs thereafter. There were no differences in the behavioral patterns and dietary intake of the animals during the experimental period.

2. Quantitative micro-CT analysis

Comparison of percentages of each parameter in quantitative micro-CT analysis among the groups are presented in Figure 12. In

the case of NBV, the PLLA－coated Mg group showed a significantly higher NBV percentage than the NC group at 4, 8, and 12 weeks (49.57 ± 8.54 vs 25.28 ± 6.66; 59.74 ± 8.55 vs 23.98 ± 6.82; and 57.88 ± 7.79 vs 26.10 ± 12.29, respectively) (all $P < 0.05$). Also, the NBV percentage in the PC group at 4 weeks (51.35 ± 2.72) was significantly higher than that in the NC group (25.28 ± 6.66) ($P < 0.05$). Other than that, no significant difference was observed among the groups in NBV.

Regarding RMV, there were no significant differences among the groups at all study periods.

In terms of TBV, results similar to those in NBV were found, and the percentage of TBV in the PLLA－coated Mg group was significantly higher than that in the NC group at 4, 8, and 12 weeks. (PLLA－coated Mg group vs NC group at 4 weeks, 72.80 ± 11.90 vs 25.32 ± 6.67; at 8 weeks, 73.75 ± 1.02 vs 24.01 ± 6.80; and at 12 weeks, 73.82 ± 12.79 vs 26.30 ± 12.56, respectively) (all $P < 0.05$).

Comparison of the residual volume and surface area of the Mg membrane between the uncoated Mg group and PLLA－coated Mg group are presented in Figure 13, and 3D reconstruction images showing the shape of residual Mg membrane in uncoated Mg and PLLA－coated Mg group at 4, 8, and 12 weeks are shown in Figure

14. Regarding the residual volume of Mg membrane, although the residual volumes in the PLLA-coated Mg group were higher than those in the uncoated Mg group at all study periods, these differences were not statistically significant. However, in the case of the residual surface area of Mg membrane, the residual surface area in the PLLA-coated Mg group was significantly higher than that in the uncoated Mg group at 4 weeks (244.26 mm^2 vs 225.31 mm^2; $P < 0.05$). At 8 and 12 weeks, there were no significant differences in residual surface area between the two groups, as in the residual volume.

3. Histological observations

Representative histological images of 4, 8, and 12 weeks for each group are presented in Figure 15 (H & E-stained) and 16 (MT-stained). In the NC group, some new bone formation was observed in a defect at 4 weeks, but the defect was mainly filled with fibrous connective tissue. Also, the center of the defect was significantly depressed, and a significant part of the original cranial architecture was lost. At 8 weeks, the bony islands and bridges filled the defect, but they were not completely connected to each other, and the vertical height of those parts was significantly lowered. At 12 weeks, the bony islands and bridges were more connected than at 8 weeks, and the vertical height was slightly uniform, but only 1/2~2/3 of the

original bone height was recovered. In addition, there were still unconnected areas between the bony islands and the bridges.

In the PC group, the space of the defect including the height at 4 weeks was well−maintained compared to the NC group. Most of the defect space was occupied by bone graft particles, but early new bone formation was observed. Such early new bone formation was observed not only at the lateral border of the defect, but also around the bone graft particles. The upper part of the defect was encapsulated by fibrous tissue, and bone graft particles protruded into some soft tissues, showing an irregular margin. At 8 weeks, mature bone structures were also observed, but fibrous tissue penetrated from the upper edge of the defect and occupied some of the defect space. In addition, as in 4 weeks, some bone graft particles protruded above the defect, forming an irregular upper margin. At 12 weeks, bone graft particles were significantly resorbed, and lamellar bone containing osteocytes was observed in many parts of the defect. However, as in 8 weeks, infiltration of soft tissue in the superior margin was observed, resulting in some loss of the upper architecture of the original defect. In addition, a large area of the bone marrow cavity was observed.

In the uncoated Mg group, at 4 weeks, soft tissue maintained at a distance from the upper edge of the defect was observed. However,

a fairly large void exists under the soft tissue, and the void area had a tendency to encroach on the upper part of the original defect architecture. As a result, some of the bone graft particles were lost, and new bone was mainly formed at the bilateral boundary of the defect although some new bones showed upward formation as if supporting soft tissue. At 8 weeks, the proportion of void area decreased compared to 4 weeks, but large void areas still existed, and void areas of rather small sizes were also scattered under the soft tissue. In addition, a large amount of MNGCs were observed in the portion presumed to be the site of the Mg membrane. In the case of new bone, mature bone was mainly observed on the lateral side of the defect, but it also started to be observed around the bone graft particles in the center. Compared to 4 weeks, the bone shape was restored as much as the original defect height, but a slight irregular boundary was formed due to the void area. At 12 weeks, an increase in mature bone accompanied by bone marrow formation was observed, but such a pattern was found to be lateral rather than central to the defect. In particular, in the lateral margin of the defect, new bone was formed right below the site where the membrane was presumed, but a large number of void areas and a significant amount of inflammatory cells and blood vessels were also observed. The large void areas that existed above the center of the defect at 4 and 8 weeks continued to

exist at 12 weeks, and the loss of bone height in the center was unavoidable.

In the PLLA－coated Mg group, new bone and bone graft particles were mixed to fill the defect, and new bone was formed in the center as well as the lateral margin of the defect at 4 weeks. In addition, abundant blood vessels were observed between the new bone and bone graft particles. Soft tissue was maintained above the presumed site of the membrane, but macrophages were present around the presumably absorbed fragments of the membrane. The large void area observed in the uncoated Mg group was also observed in the PLLA－coated Mg group, but the distribution of the void area was smaller and the loss of the original vertical height was also less. At 8 weeks, the lateral mature bone and the mature bone and bone graft particles in the central part were connected, and the original defect contour was well－maintained overall. However, the large void area became wider than at 4 weeks. Nevertheless, the contour of the upper edge of the defect was well－maintained due to the widely distributed new bone and supporting bone graft particles. In addition, fewer MNGCs were observed around the site where the membrane was presumed to be present compared to the uncoated Mg group. At 12 weeks, the new mature bone and the remaining bone graft particles were more closely connected overall, and the original defect

architecture was completely restored. Furthermore, properly formed bone marrow and blood vessels began to be observed. The void area above the healed defect was still present, but the distribution range was significantly reduced and a linear shape of void was observed. As in 8 weeks, MNGCs were observed, but still only a small amount was observed around the presumed fragments of membrane.

4. Histomorphometric analysis

Comparison of the percentages of NBA, RMA, and TBA by histomorphometric analysis among the groups are shown in Figure 17. In the case of the percentage of NBA, there were no significant differences among the groups at all study periods.

Regarding the percentage of RMA, the PLLA-coated Mg group showed the highest percentage of RMA among all groups at 8 and 12 weeks, but the differences were not statistically significant.

In terms of the percentage of TBA, the PLLA-coated Mg group showed the highest percentage among all groups at all study periods, but the differences were not statistically significant.

Comparison of inflammatory response scores and the numbers of MNGCs among the groups are presented in Figure 18. Inflammatory response scores showed significant differences between the PC group and the uncoated Mg group at all study periods, and the score

of uncoated Mg group was higher than that of the PC group. (uncoated Mg group vs PC group at 4 weeks, 2.75 ± 0.50 vs 0.25 ± 0.50; uncoated Mg group vs PC group at 8 weeks, 3.75 ± 0.50 vs 0.50 ± 0.58; and uncoated Mg group vs PC group at 12 weeks, 4.00 ± 0.82 vs 0.25 ± 0.50, respectively) (at 4 and 8 weeks, $P < 0.05$; and at 12 weeks, $P < 0.01$, respectively).

Regarding the number of MNGCs, the number of MNGCs in uncoated Mg group was the highest among all groups at 4 and 8 weeks, but the differences were not statistically significant. In contrast, at 12 weeks, the number of MNGCs in PLLA−coated Mg group was the highest among all groups, but the difference was not statistically significant.

5. Immunohistochemical analysis

Comparison of the percentage of OC and OPN expression among the groups are shown in Figure 19, and representative immunohistochemical images of 4, 8, and 12 weeks for each group are presented in Figure 20 (OC expression) and 21 (OPN expression). Although OC and OPN were weakly expressed around the new bone, they showed a tendency to be strongly expressed mainly around Bio−Oss® (Figure 22). In the case of the percentage of OC expression, the uncoated Mg group showed a significantly

higher percentage than the NC group at 4 weeks (18.52 ± 7.80 vs 0.00 ± 0.00; $P < 0.05$), whereas the percentage of the PLLA−coated Mg group was significantly higher than that of the NC group at 8 weeks (4.67 ± 6.13 vs 0.00 ± 0.00; $P < 0.05$). At 12 weeks, both the uncoated Mg group and the PLLA−coated Mg group showed significantly higher percentages than the NC group (uncoated Mg group vs NC group, 4.03 ± 1.83 vs 0.00 ± 0.00; and PLLA−coated Mg group vs NC group, 5.41 ± 3.09 vs 0.00 ± 0.00, respectively) (both $P < 0.05$).

Regarding the percentage of OPN expression, at 4 weeks, only the percentage of the PLLA−coated Mg group was higher than that of the NC group (26.05 ± 2.54 vs 0.00 ± 0.00; $P < 0.05$), but at 8 and 12 weeks, both the PLLA−coated Mg group and the uncoated Mg group showed a higher percentage than the NC group (PLLA−coated Mg group vs NC group at 8 weeks, 11.59 ± 8.04 vs 0.00 ± 0.01; uncoated Mg group vs NC group at 8 weeks, 17.71 ± 14.41 vs 0.00 ± 0.01; PLLA−coated Mg group vs NC group at 12 weeks, 11.17 ± 10.36 vs 0.00 ± 0.00; and uncoated Mg group vs NC group at 12 weeks, 6.02 ± 3.61 vs 0.00 ± 0.00, respectively) (all $P < 0.05$).

Discussion

The present study investigated the safety and efficacy of PLLA-coated Mg membrane in GBR through *in vitro* and *in vivo* tests. In the case of safety including biocompatibility of PLLA-coated Mg membrane, it was considered that Mg membrane with or without coating showed no cytotoxic effect because grade 0 of qualitative morphological grading of cytotoxicity of extracts in ISO 10993-5 was achieved (Table 1). Also, in the MTT assay, the cell viability of the PLLA-coated Mg membrane did not indicate the cytotoxic potential (Figure 11). In the *in vivo* test using a rabbit calvarium model, the PLLA-coated Mg group did not show a significant difference from the NC and PC groups in inflammatory response scores in histomorphometric analysis (Figure 18), and did not reveal any significant inflammatory signs in clinical evaluation. In terms of the effectiveness of the PLLA-coated Mg membrane, it was observed that the PLLA-coated Mg membrane degraded more slowly and maintained its shape for a longer time compared to the uncoated Mg membrane through *in vitro* degradation test (Figure 8 and 9) and micro-CT analysis of *in vivo* test (Figure 13 and 14). Furthermore, the PLLA-coated group had the highest TBA percentage at all study periods, and the RMA percentage in PLLA-coated Mg group was highest among all groups at 8 and 12 weeks (Figure 17). In micro-CT analysis, the PLLA-coated group showed the highest percentage

of TBV and NBV at 8 and 12 weeks, and those of the coated group were statistically significantly higher than those of the negative control group (both $P < 0.05$) (Figure 12). Therefore, in light of the above results, it is considered that PLLA-coated Mg membrane has safety and efficacy in GBR at both *in vitro* and *in vivo* levels. For clinical use of PLLA-coated Mg membrane in the future, the possibility of conducting clinical trials by accumulating the results of additional studies including the present study should be evaluated.

Mg and its alloy are being applied to stents,[33-36] plates and screws[37-41] in various fields due to their excellent biocompatibility and biodegradability. Efforts to fabricate membranes made of Mg and its alloys for GBR and verify their biocompatibility and efficacy have begun as well, focusing on the advantages of Mg and its alloys. In order to overcome the known limitations of the pure Mg membrane such as corrosion and the resulting hydrogen gas generation, some studies have been conducted to confirm delay of biodegradation, and osteogenic ability by modifying the alloy composition of the Mg membrane or coating the surface of the Mg membrane with various materials.[42-46] In a study investigating the *in vitro* physiobiological properties and *in vivo* regenerative performance of a membrane made of Mg-Zn-Gd alloy with or without calcium phosphate (Ca-P) coating,[45] Mg-Zn-Gd membrane with Ca-P coating reduced the

3 0

degradation rate compared to uncoated Mg-Zn-Gd membrane although it could not prevent unsatisfying early gas formation. In addition, Mg-Zn-Gd membrane with or without Ca-P coating showed excellent mechanical properties and good biocompatibility. Peng *et al.* [44] also applied Ca-P coating to the membrane. However, in contrast to the study described above, Peng *et al.*[44] applied the coating to pure Mg membrane, and investigated its feasibility in GBR. They performed their study on the basis of the fact that Ca-P coating has non-toxicity and can enhance the biocompatibility of the substrate used as the implants,[47] and Ca-P coating showed increased corrosion resistance of pure Mg membrane *in vitro* and *in vivo*. As another coating material for Mg membrane, hydroxyapatite (HA) and chitosan were studied. In the case of HA, paying attention to its well-known biocompatibility and osteoconductivity, Byun *et al.*[42] used HA-coated Mg mesh for calvarial defects in rats to investigate the possibility of its use in GBR. However, there was no significant difference in bone formation between the control group and the experimental group in which HA-coated mesh was used, and it was concluded that the effectiveness of HA-coated Mg mesh in GBR should be reconsidered. As for chitosan, a natural resorbable polymer, research was conducted based on its excellent biological properties and known ability to slow the degradation rate of Mg alloys.[48,49] Guo

3 1

et al.[43] performed *in vitro* and *in vivo* tests by applying chitosan coating to a membrane made of Mg alloy containing Gd, and the chitosan-coated Mg membrane showed suitable degradation and good biocompatibility *in vitro* and improved bone regeneration *in vivo*. Steigmann *et al.*[46] performed a coating method called physical vapor deposition (PVD) to produce a chromium-nitrogen layer on the outer layer of the Mg membrane. PVD coating technique was mainly used to improve mechanical and tribological properties in surgical instruments, and was applied with the expectation that corrosion resistance could be improved in Mg membrane as well. However, contrary to expectations, the PVD-coated membrane showed no cytocompatible results *in vitro* and did not affect the gas cavity formation according to a study by Steigmann *et al.*[46] As described above, in studies for the development of Mg membrane for GBR, the method of applying various coating materials rather than modifying the alloy composition is mainstream. In the present study, *in vitro* and *in vivo* tests were performed by PLLA coating on Mg membrane containing Dy, and the favorable biocompatibility and efficacy of PLLA-coated Mg membrane in GBR were confirmed.

Substantial investigations have shown that surface coating of Mg-based materials to increase corrosion resistance is a satisfactory strategy. The coating layer prevents the substrates from contacting

the corrosive agents, thus allowing a significant delay in the initial corrosion process.[17] In addition, it is easy and time-saving compared to complex alloying techniques. PLLA used in the present study is a kind of resorbable synthetic polymer, and the degradation process is more controllable than natural polymers such as chitosan or gelatin. Because synthetic polymers including PLLA can be easily modified according to the needs for biomedical applications,[50] they are expected to be promising coating agents for Mg-based materials in tissue engineering. Zhu *et al.*[51] applied PLLA coating to pure Mg substrate, and reported cytocompatibility and delayed corrosion rate as a result of *in vitro* tests. Sheng *et al.*[52] also performed PLLA coating to Mg rods for improvement of corrosion resistance in biological fluids, and reported significantly improved corrosion resistance and suppressed corrosion rate of substrates through electrochemical corrosion test and immersion test. In the field of cardiology, Magmaris scaffold (Biotronik AG, Buelach, Switzerland), which has been actively studied as a resorbable Mg scaffold and has been limitedly used in clinical trials, is made by applying a PLLA coating to WE43 [Mg-yttrium (Y)-Nd-Zr] alloy. Its safety and effectiveness as an Mg-based scaffold have been demonstrated through preclinical and clinical studies.[53-56] However, Resoloy®, which was developed as an alternative alloy to WE43, is also

completely resorbed in the tissue and exhibits slightly better mechanical properties than WE43,[57] so its potential as a new material has emerged. Menze and Wittchow's research[57] is the only study that tested the application of PLLA coating to Resoloy® alloy in an *in vivo* study although PLLA coating as well as fluoride passivation layer were applied to the Resoloy®. As a preclinical study, they applied a fluoride passivation layer with or without PLLA coating to the Resoloy®, and investigated its feasibility, safety and absorption in a coronary porcine model. As a result, compared to applying only the fluoride passivation layer to the Resoloy®, when the PLLA coating was also applied, the structural integrity and stability were longer and both surface modification showed favorable safety.[57] Based on this results, an *in vivo* test was performed by applying PLLA coating to the membrane made of Resoloy® in the present study for GBR as well, and the results that the coated Mg membrane retains its shape for a longer period of time and has good safety are consistent with the study of Menze and Wittchow.[57]

Since the duration of the integrity of the resorbable membrane is related to the space-maintaining ability, it is an important factor in GBR. For guided tissue generation, cells required for regeneration undergo maturation at the wound sites within approximately 3-4 weeks.[58] Based on this, the membrane for periodontal tissue

3 4

generation should be maintained for 4-6 weeks, whereas a longer period of 16-24 weeks is recommended for bone regeneration.[59] However, despite these recommendations, the ideal period of retaining the barrier function of membrane for optimal healing results has not yet been accurately determined.[60] In the present study, it was observed that both uncoated Mg and coated Mg membrane remained up to 12 weeks on micro-CT analysis except for one rabbit who showed swelling 1-2 weeks after surgery. Although there was a statistically significant difference only in the residual surface area between the two groups at 4 weeks, the residual volume and residual surface area of the coated Mg membrane were higher than those of the uncoated Mg membrane at all experimental period. Therefore, it is carefully assumed that the PLLA-coated Mg membrane may exhibit a slower absorption compared to the uncoated Mg membrane, and its shape may be maintained for a longer time compared to that of the uncoated Mg membrane. To the best of author's knowledge, the present study is the first study to measure the residual volume and surface area of Mg membrane in an *in vivo* study using micro-CT, so it is difficult to compare with the results of other studies. For measurement of the volume and surface area of the residual Mg membrane with or without PLLA-coating, a cross-sectional image in 3D reconstruction was used to designate and measure the area for

each cross-section one by one. Since this process is rather time-consuming, it is presumed that it has not been attempted in other studies. In order to measure the residual amount of Mg membrane more accurately, it was also necessary to measure the parameters of the residual Mg membrane using histomorphometric analysis, but this analysis was not possible in the present study because the form of the membrane was lost by acid during the decalcification process on the specimen. Measurement of the amount of residual membrane through histomorphometric analysis should be attempted without the decalcification process, and additional research is needed.

Non-collagenous bone matrix protein, which is present in only a small amount of organics constituting about 33% of bone, plays an important role in bone quality.[61] Among these bone matrix proteins, OC and OPN are known to be critically involved in the biological function of bone.[62] OC is a protein expressed in the late stage of bone differentiation and induces calcification of bone tissue by binding with HA and calcium ions.[63] OPN is known to promote adhesion and migration of cells involved in bone metabolism to bone tissue and increases bone mineralization.[64,65] In a previous study of the immunohistochemical expression of OC and OPN in GBR sites,[66] it was found that OC and OPN were present in high concentrations under the collagen membrane. Thus, these markers are also expected

to provide the evaluation of the impact of resorbable Mg−based implants on different stages of bone formation through their expression.[67] Therefore, the expression rates of OC and OPN were evaluated in the present study through immunodetection to further investigate the pattern of osteogenesis when using Mg membrane with or without PLLA coating in GBR. As result, both OC and OPN showed the highest expression percentage at week 4 in all groups except NC group, and thereafter, the expression percentage showed a decreasing pattern. In the case of NC group, both OC and OPN expression rates were very low in all study periods, but they did not actually show a value of 0. In the comparison among each group, the expression rate of OC and OPN showed slightly different results among groups. At 4 weeks, in the case of OC, only the uncoated Mg group showed a significantly higher expression percentage than the NC group, whereas, in the case of OPN, only the PLLA−coated Mg group showed a significantly higher expression percentage than the NC group. At 8 weeks, the PLLA−coated Mg group showed a higher percentage of OC expression than the NC group, and both the uncoated and PLLA−coated Mg group showed a higher percentage of OPN expression than the NC group. At 12 weeks, both uncoated and PLLA−coated Mg groups showed higher expression percentages of OC and OPN compared to the NC group. Consequently, as time passes,

it is thought that the expression percentage of OC and OPN in the groups to which the Mg membrane was applied tended to be higher than that in the groups to which the membrane was not applied although the difference was not much and the absolute amount was reduced. The reason why the expression rates of OC and OPN were higher at 4 weeks in the present study may be explained by the result of other study in which immunopositivity of OC and OPN started to appear from 2 weeks to induce osteoblast differentiation.[66] Therefore, it is thought that the expression percentage of OC and OPN was rather high at 4 weeks, which is considered to be the initial healing period, to induce osteoblast differentiation for new bone formation. In addition, in light of one study that reported bone formation in a rabbit calvarial model reached a peak about 40 days (5-6 weeks) after surgery and entered the remodeling phase thereafter,[68] it might be estimated that the expression percentage of OC and OPN would decrease at 8 and 12 weeks postoperatively. Nevertheless, the PLLA-coated Mg group showed higher OC and OPN expression percentages compared to the NC group at 8 and 12 weeks, so it is thought that it would induce new bone formation for a longer period. This inference might be supported by the result showing a higher new bone volume percentage in the PLLA-coated Mg group than in the NC group in the micro-CT analysis (Figure 12).

One of the unexpected results observed in the present study was that the Mg membrane with or without coating remained after 12 weeks. In a study using pure Mg membrane with or without calcium−phosphate coating in a rabbit calvarial defect,[45] no membrane was observed at 8 weeks. Also, in the study using chitosan−coated Mg membrane in the same model,[43] no membrane was left at 12 weeks. Therefore, it was estimated that all Mg membranes would be absorbed within 12 weeks in the present study, but it was observed that some of the uncoated Mg membranes as well as the coated Mg membranes remained until 12 weeks. This difference is presumed to be due to the difference in composition of Mg alloy and coating material. Another unexpected result was that there were few clinical signs associated with hydrogen gas formation. Although one rabbit with uncoated Mg membrane showed tissue swelling above the wound for up to 2 weeks postoperatively, the other rabbits did not show any signs. In addition, the rabbit's edema was subsided without any additional medication or treatment. When considering the results of other studies, the reports related to clinical signs are rather mixed. One study showed that a subcutaneous gas pocket was observed in all rabbits for a week,[44] while others reported no specific inflammatory response in clinical observation.[45,69] In the present study, a slightly convex Mg membrane was used, so there was a

space that did not completely contact the bone graft material in the defect and calvarial bone in the lateral part of the defect. Thus, it is presumed that the hydrogen gas generated due to corrosion was collected in this space, and the histological findings that large void areas were observed in the area below the membrane support this assumption. In addition, since the Mg membrane used in the present study has a mesh design, it cannot be excluded that it facilitated the movement of gas below the membrane. Consequently, it is thought that the hydrogen gas did not migrate above the membrane due to these possibilities, and did not cause the related clinical signs. Further studies are needed to elucidate these points.

The present study differs from other studies in several respects. First, this is the first study to conduct both *in vitro* and *in vivo* tests by fabricating a barrier membrane for GBR using Mg alloy coated with PLLA. Second, the present study performed immunohistochemical analysis using OC and OPN in addition to micro-CT analysis and histomorphometric analysis not only to confirm the ability of bone formation or bone maintenance but also to investigate the expression and activity of bone matrix proteins in performance of Mg membrane. Third, the present study measured the surface area and volume of the remaining Mg membrane through micro-CT analysis, and was able to compare the residual amount of the uncoated membrane and

the coated membrane. Currently, there is no study measuring the residual amount of Mg membrane in the rabbit skull model by micro–CT. Lastly, besides the NC group, the PC group and the uncoated Mg membrane group were set, and the experiment was designed to further identify the difference between them and the PLLA–coated Mg membrane group. In addition, since the analyses were conducted according to three experimental periods as early (4 weeks), intermediate (8 weeks), and late (12 weeks) time points, it was possible to evaluate the performance and absorption patterns of the Mg membrane with or without PLLA coating for each period. Considering other studies that applied Mg membrane in the rabbit calvarial model were conducted by dividing the experimental period into only 6 and 12 weeks,[43,45] the above can be an advantage of the present study.

Although the present study is the first study to evaluate Mg membrane with PLLA coating for GBR, there are several limitations in the present study. In the investigation of resorbable Mg alloy for clinical application, it is important to evaluate the generation of hydrogen gas related to corrosion of Mg alloy because gas cavities are formed at the wound site, and related signs such as wound dehiscence, inflammation, and edema may appear. For this reason, it is necessary to quantitatively measure the amount of hydrogen gas

generated by corrosion of Mg alloy or the gas cavity associated with it. In the present study, it was attempted to measure the area of the cavity (void area) created by hydrogen gas, but it was not possible. The reason is that the Mg membrane and the outer layer of Bio-Oss® disappeared due to the demineralization process for the preparation of histological specimens, creating a transparent area, which was difficult to distinguish from the void caused by hydrogen gas. Although there were no specific findings except for one rabbit with edema during clinical observation, the difference in the absorption rate between the uncoated membrane and the coated membrane could not be evaluated through quantitative comparison of gas cavity formation. In addition, it should have been observed for a long-term period until the Mg membrane with or without coating was completely absorbed, but it was not possible due to the unexpectedly long remaining period of the membrane. Finally, as a limitation related to the fixation and adaptation of the Mg membrane, there was no screw to fix the membrane, and no manipulation was performed to adhere to the bone surface. An attempt was made to fabricate Mg screws to fix the Mg membrane, but at that point, only titanium screws were available, and Mg screws of the same size were impossible to manufacture. Therefore, the use of titanium screws was considered, but according to the research result that corrosion was accelerated

when Mg and titanium were co-implanted,[70] it was decided to proceed with the experiment without using a screw. In addition, due to the convexity caused by the fabrication of PLLA-coated Mg membrane, manipulation for close adaptation was required for GBR procedure in the present study. However, Mg membranes were used without additional manipulation to minimize the damage to the coating layer. In future studies, the study design is required to quantitatively measure the amount of hydrogen gas due to corrosion of Mg for a longer study period. Furthermore, additional studies should be conducted considering the effective fixation and free manipulation of the Mg membrane.

Conclusions

The present study investigated the safety and efficacy of Mg membrane with PLLA coating for GBR through *in vitro* and *in vivo* tests. Regarding the safety, PLLA-coated Mg membrane showed favorable biocompatibility through *in vitro* cytotoxicity test and *in vivo* test. In terms of efficacy, PLLA-coated Mg membrane showed delayed degradation through *in vitro* degradation test and *in vivo* test, and also showed good bone formation and maintenance ability. Therefore, it is considered that PLLA-coated Mg membrane has

safety and efficacy in GBR at both *in vitro* and *in vivo* levels. Further studies are needed for the development of a resorbable Mg membrane with PLLA－coating and its clinical application.

References

1. Cho KS, Choi SH, Han KH, Chai JK, Wikesjo UM, Kim CK: Alveolar bone formation at dental implant dehiscence defects following guided bone regeneration and xenogeneic freeze-dried demineralized bone matrix. Clin Oral Implants Res 1998;9:419-28.

2. Simion M. Horizontal and vertical bone volume augmentation of implant sites using guided bone regeneration (GBR) Proceedings of the 3rd European Workshop on Periodontology, Quintessence Pub. Co. 1999:500-19.

3. Klokkevold PR, Newman MG: Current status of dental implants: a periodontal perspective. Int J Oral Maxillofac Implants 2000;15:56-65.

4. Briguglio F, Falcomatà D, Marconcini S, Fiorillo L, Briguglio R, Farronato D: The use of titanium mesh in guided bone regeneration: a systematic review. Int J Dent 2019;2019:9065423.

5. Walker J, Shadanbaz S, Woodfield TB, Staiger MP, Dias GJ: Magnesium biomaterials for orthopedic application: a review from a biological perspective. J Biomed Mater Res B Appl Biomater 2014;102:1316-31.

6. Meng J, Sun W, Tian Z, Qiu X, Zhang D. 2—corrosion performance of magnesium (Mg) alloys containing rareearth (RE) elements. Corrosion Prevention of Magnesium Alloys, Woodhead Pub. 2013:38-60.

7.	Hort N, Huang Y-d, Fechner D, Störmer M, Blawert C, Witte F, *et al.*: Magnesium alloys as implant materials-Principles of property design for Mg-RE alloys. Acta Biomater 2010;6:1714-25.

8.	Liu D, Yang D, Li X, Hu S: Mechanical properties, corrosion resistance and biocompatibilities of degradable Mg-RE alloys: A review. J Mater Res Technol 2019;8:1538-49.

9.	Byun SH, Lim HK, Cheon KH, Lee SM, Kim HE, Lee JH: Biodegradable magnesium alloy (WE43) in bone-fixation plate and screw. J Biomed Mater Res B Appl Biomater 2020;108:2505-12.

10.	Schaller B, Matthias Burkhard JP, Chagnon M, Beck S, Imwinkelried T, Assad M: Fracture Healing and Bone Remodeling With Human Standard-Sized Magnesium Versus Polylactide-Co-Glycolide Plate and Screw Systems Using a Mini-Swine Craniomaxillofacial Osteotomy Fixation Model. J Oral Maxillofac Surg 2018;76:2138-50.

11.	Torroni A, Xiang C, Witek L, Rodriguez ED, Flores RL, Gupta N, *et al.*: Histo-morphologic characteristics of intra-osseous implants of WE43 Mg alloys with and without heat treatment in an in vivo cranial bone sheep model. J Craniomaxillofac Surg 2018;46:473-8.

12.	Feyerabend F, Fischer J, Holtz J, Witte F, Willumeit R, Drucker H, *et al.*: Evaluation of short-term effects of rare earth and other elements used in magnesium alloys on primary cells and cell lines. Acta Biomater 2010;6:1834-42.

13.	Yang L, Huang Y, Feyerabend F, Willumeit R, Mendis C, Kainer KU,

et al.: Microstructure, mechanical and corrosion properties of Mg−Dy−Gd−Zr alloys for medical applications. Acta Biomater 2013;9:8499−508.

14. Maier P, Steinacker A, Clausius B, Hort N: Influence of solution heat treatment on the microstructure, hardness and stress corrosion behavior of extruded Resoloy®. JOM 2020;72:1870−9.

15. Alvarez−Lopez M, Pereda MD, del Valle JA, Fernandez−Lorenzo M, Garcia−Alonso MC, Ruano OA, *et al.*: Corrosion behaviour of AZ31 magnesium alloy with different grain sizes in simulated biological fluids. Acta Biomater 2010;6:1763−71.

16. Wong HM, Yeung KW, Lam KO, Tam V, Chu PK, Luk KD, *et al.*: A biodegradable polymer−based coating to control the performance of magnesium alloy orthopaedic implants. Biomaterials 2010;31:2084−96.

17. Zhu Y, Liu W, Ngai T: Polymer coatings on magnesium-based implants for orthopedic applications. J Polym Sc 2022;60:32−51.

18. Ma J, Thompson M, Zhao N, Zhu D: Similarities and differences in coatings for magnesium−based stents and orthopaedic implants. J Orthop Translat 2014;2:118−30.

19. Wang J, Tang J, Zhang P, Li Y, Wang J, Lai Y, *et al.*: Surface modification of magnesium alloys developed for bioabsorbable orthopedic implants: a general review. J Biomed Mater Res B Appl Biomater 2012;100:1691−701.

20. Jiang Y, Wang B, Jia Z, Lu X, Fang L, Wang K, *et al.*: Polydopamine

mediated assembly of hydroxyapatite nanoparticles and bone morphogenetic protein-2 on magnesium alloys for enhanced corrosion resistance and bone regeneration. J Biomed Mater Res A 2017;105:2750-61.

21. Li LY, Cui LY, Zeng RC, Li SQ, Chen XB, Zheng Y, *et al.*: Advances in functionalized polymer coatings on biodegradable magnesium alloys - A review. Acta Biomater 2018;79:23-36.

22. Yin Z-Z, Qi W-C, Zeng R-C, Chen X-B, Gu C-D, Guan S-K, *et al.*: Advances in coatings on biodegradable magnesium alloys. J Magnes Alloy 2020;8:42-65.

23. Abdal-Hay A, Dewidar M, Lim J, Lim JK: Enhanced biocorrosion resistance of surface modified magnesium alloys using inorganic/organic composite layer for biomedical applications. Ceram Int 2014;40:2237-47.

24. Chen J-Y, Chen X-B, Li J-L, Tang B, Birbilis N, Wang X: Electrosprayed PLGA smart containers for active anti-corrosion coating on magnesium alloy AMlite. J Mater Chem A 2014;2:5738-43.

25. Ostrowski NJ, Lee B, Roy A, Ramanathan M, Kumta PN: Biodegradable poly(lactide-co-glycolide) coatings on magnesium alloys for orthopedic applications. J Mater Sci Mater Med 2013;24:85-96.

26. Zeng RC, Cui LY, Jiang K, Liu R, Zhao BD, Zheng YF: In Vitro Corrosion and Cytocompatibility of a Microarc Oxidation Coating and

Poly(L-lactic acid) Composite Coating on Mg-1Li-1Ca Alloy for Orthopedic Implants. ACS Appl Mater Interfaces 2016;8:10014-28.

27. Zhang L, Pei J, Wang H, Shi Y, Niu J, Yuan F, *et al.*: Facile Preparation of Poly(lactic acid)/Brushite Bilayer Coating on Biodegradable Magnesium Alloys with Multiple Functionalities for Orthopedic Application. ACS Appl Mater Interfaces 2017;9:9437-48.

28. Pihlajamaki H, Bostman O, Hirvensalo E, Tormala P, Rokkanen P: Absorbable pins of self-reinforced poly-L-lactic acid for fixation of fractures and osteotomies. J Bone Joint Surg Br 1992;74:853-7.

29. Schumann P, Lindhorst D, Wagner ME, Schramm A, Gellrich NC, Rucker M: Perspectives on resorbable osteosynthesis materials in craniomaxillofacial surgery. Pathobiology 2013;80:211-7.

30. Kao ST, Scott DD: A review of bone substitutes. Oral Maxillofac Surg Clin North Am 2007;19:513-21, vi.

31. Meijndert L, Raghoebar GM, Schupbach P, Meijer HJ, Vissink A: Bone quality at the implant site after reconstruction of a local defect of the maxillary anterior ridge with chin bone or deproteinised cancellous bovine bone. Int J Oral Maxillofac Surg 2005;34:877-84.

32. Yildirim M, Spiekermann H, Handt S, Edelhoff D: Maxillary sinus augmentation with the xenograft Bio-Oss and autogenous intraoral bone for qualitative improvement of the implant site: a histologic and histomorphometric clinical study in humans. Int J Oral Maxillofac Implants 2001;16:23-33.

33. Charpentier E, Barna A, Guillevin L, Juliard JM: Fully bioresorbable

drug-eluting coronary scaffolds: A review. Arch Cardiovasc Dis 2015;108:385-97.

34. Sotomi Y, Onuma Y, Collet C, Tenekecioglu E, Virmani R, Kleiman NS, *et al.*: Bioresorbable Scaffold: The Emerging Reality and Future Directions. Circ Res 2017;120:1341-52.

35. Tenekecioglu E, Farooq V, Bourantas CV, Silva RC, Onuma Y, Yilmaz M, *et al.*: Bioresorbable scaffolds: a new paradigm in percutaneous coronary intervention. BMC Cardiovasc Disord 2016;16:38.

36. Luffy SA, Chou DT, Waterman J, Wearden PD, Kumta PN, Gilbert TW: Evaluation of magnesium-yttrium alloy as an extraluminal tracheal stent. J Biomed Mater Res A 2014;102:611-20.

37. Biber R, Pauser J, Brem M, Bail HJ: Bioabsorbable metal screws in traumatology: A promising innovation. Trauma Case Rep 2017;8:11-5.

38. Leonhardt H, Franke A, McLeod NMH, Lauer G, Nowak A: Fixation of fractures of the condylar head of the mandible with a new magnesium-alloy biodegradable cannulated headless bone screw. Br J Oral Maxillofac Surg 2017;55:623-5.

39. Liu C, Ren Z, Xu Y, Pang S, Zhao X, Zhao Y: Biodegradable Magnesium Alloys Developed as Bone Repair Materials: A Review. Scanning 2018;2018:9216314.

40. Naujokat H, Seitz JM, Acil Y, Damm T, Moller I, Gulses A, *et al.*: Osteosynthesis of a cranio-osteoplasty with a biodegradable magnesium plate system in miniature pigs. Acta Biomater

2017;62:434-45.

41. Zhao D, Witte F, Lu F, Wang J, Li J, Qin L: Current status on clinical applications of magnesium-based orthopaedic implants: A review from clinical translational perspective. Biomaterials 2017;112:287-302.

42. Byun SH, Lim HK, Kim SM, Lee SM, Kim HE, Lee JH: The Bioresorption and Guided Bone Regeneration of Absorbable Hydroxyapatite-Coated Magnesium Mesh. J Craniofac Surg 2017;28:518-23.

43. Guo Y, Yu Y, Han L, Ma S, Zhao J, Chen H, *et al.*: Biocompatibility and osteogenic activity of guided bone regeneration membrane based on chitosan-coated magnesium alloy. Mater Sci Eng C Mater Biol Appl 2019;100:226-35.

44. Peng W, Chen J-X, Shan X-F, Wang Y-C, He F, Wang X-J, *et al.*: Mg-based absorbable membrane for guided bone regeneration (GBR): a pilot study. Rare Metals 2019;38:577-87.

45. Si J, Shen H, Miao H, Tian Y, Huang H, Shi J, *et al.*: In vitro and in vivo evaluations of Mg-Zn-Gd alloy membrane on guided bone regeneration for rabbit calvarial defect. J Magnes Alloy 2021;9:281-91.

46. Steigmann L, Jung O, Kieferle W, Stojanovic S, Proehl A, Gorke O, *et al.*: Biocompatibility and Immune Response of a Newly Developed Volume-Stable Magnesium-Based Barrier Membrane in Combination with a PVD Coating for Guided Bone Regeneration

(GBR). Biomedicines 2020;8.

47. Elgali I, Turri A, Xia W, Norlindh B, Johansson A, Dahlin C, *et al.*: Guided bone regeneration using resorbable membrane and different bone substitutes: Early histological and molecular events. Acta Biomater 2016;29:409-23.

48. Hahn B-D, Park D-S, Choi J-J, Ryu J, Yoon W-H, Choi J-H, *et al.*: Aerosol deposition of hydroxyapatite-chitosan composite coatings on biodegradable magnesium alloy. Surf Coat Technol 2011;205:3112-8.

49. Jun Z, Chen L-j, Kun Y, Chang C, Dai Y-l, Qiao X-y, *et al.*: Effects of chitosan coating on biocompatibility of Mg-6% Zn-10% Ca3 (PO4) 2 implant. Trans Nonferrous Met Soc China 2015;25:824-31.

50. Song R, Murphy M, Li C, Ting K, Soo C, Zheng Z: Current development of biodegradable polymeric materials for biomedical applications. Drug Des Devel Ther 2018;12:3117-45.

51. Zhu Y, Zheng L, Liu W, Qin L, Ngai T: Poly(l-lactic acid) (PLLA)/MgSO4.7H2O Composite Coating on Magnesium Substrates for Corrosion Protection and Cytocompatibility Promotion. ACS Appl Bio Mater 2020;3:1364-73.

52. Sheng Y, Tian L, Wu C, Qin L, Ngai T: Biodegradable Poly(l-lactic acid) (PLLA) Coatings Fabricated from Nonsolvent Induced Phase Separation for Improving Corrosion Resistance of Magnesium Rods in Biological Fluids. Langmuir 2018;34:10684-93.

53. Garcia-Garcia HM, Haude M, Kuku K, Hideo-Kajita A, Ince H,

Abizaid A, *et al.*: In vivo serial invasive imaging of the second-generation drug-eluting absorbable metal scaffold (Magmaris - DREAMS 2G) in de novo coronary lesions: Insights from the BIOSOLVE-II First-In-Man Trial. Int J Cardiol 2018;255:22-8.

54. Haude M, Erbel R, Erne P, Verheye S, Degen H, Vermeersch P, *et al.*: Safety and performance of the DRug-Eluting Absorbable Metal Scaffold (DREAMS) in patients with de novo coronary lesions: 3-year results of the prospective, multicentre, first-in-man BIOSOLVE-I trial. EuroIntervention 2016;12:e160-6.

55. Joner M, Ruppelt P, Zumstein P, Lapointe-Corriveau C, Leclerc G, Bulin A, *et al.*: Preclinical evaluation of degradation kinetics and elemental mapping of first- and second-generation bioresorbable magnesium scaffolds. EuroIntervention 2018;14:e1040-e8.

56. Waksman R, Zumstein P, Pritsch M, Wittchow E, Haude M, Lapointe-Corriveau C, *et al.*: Second-generation magnesium scaffold Magmaris: device design and preclinical evaluation in a porcine coronary artery model. EuroIntervention 2017;13:440-9.

57. Menze R, Wittchow E: In vitro and in vivo evaluation of a novel bioresorbable magnesium scaffold with different surface modifications. J Biomed Mater Res B Appl Biomater 2021;109:1292-302.

58. Iglhaut J, Aukhil I, Simpson DM, Johnston MC, Koch G: Progenitor cell kinetics during guided tissue regeneration in experimental periodontal wounds. J Periodontal Res 1988;23:107-17.

59. Caballe-Serrano J, Abdeslam-Mohamed Y, Munar-Frau A, Fujioka-Kobayashi M, Hernandez-Alfaro F, Miron R: Adsorption and release kinetics of growth factors on barrier membranes for guided tissue/bone regeneration: A systematic review. Arch Oral Biol 2019;100:57-68.

60. Kim SH, Kim DY, Kim KH, Ku Y, Rhyu IC, Lee YM: The efficacy of a double-layer collagen membrane technique for overlaying block grafts in a rabbit calvarium model. Clin Oral Implants Res 2009;20:1124-32.

61. Morgan S, Poundarik AA, Vashishth D: Do Non-collagenous Proteins Affect Skeletal Mechanical Properties? Calcif Tissue Int 2015;97:281-91.

62. Olszta MJ, Cheng X, Jee SS, Kumar R, Kim Y-Y, Kaufman MJ, et al.: Bone structure and formation: A new perspective. Mater Sci Eng R Rep 2007;58:77-116.

63. Mundy GR, Martin TJ. Physiology and pharmacology of bone. Springer 1993:641-71.

64. Chen J, Singh K, Mukherjee BB, Sodek J: Developmental expression of osteopontin (OPN) mRNA in rat tissues: evidence for a role for OPN in bone formation and resorption. Matrix 1993;13:113-23.

65. Goldberg HA, Warner KJ, Li MC, Hunter GK: Binding of bone sialoprotein, osteopontin and synthetic polypeptides to hydroxyapatite. Connect Tissue Res 2001;42:25-37.

66. Taguchi Y, Amizuka N, Nakadate M, Ohnishi H, Fujii N, Oda K, et al.:

A histological evaluation for guided bone regeneration induced by a collagenous membrane. Biomaterials 2005;26:6158-66.

67. Bondarenko A, Angrisani N, Meyer-Lindenberg A, Seitz JM, Waizy H, Reifenrath J: Magnesium-based bone implants: immunohistochemical analysis of peri-implant osteogenesis by evaluation of osteopontin and osteocalcin expression. J Biomed Mater Res A 2014;102:1449-57.

68. Gulinelli JL, Queiroz TP, Hochuli-Vieira E, Okamoto R, Mattos JMB, Calcagnotto T, et al.: Use of Calcium Phosphate Cement for Repairing Bone Defects: Histomorphometric and Immunohistochemical Analyses. J Craniofac Surg 2019;30:1016-21.

69. Rider P, Kacarevic ZP, Elad A, Tadic D, Rothamel D, Sauer G, et al.: Biodegradable magnesium barrier membrane used for guided bone regeneration in dental surgery. Bioact Mater 2022;14:152-68.

70. Hou P, Han P, Zhao C, Wu H, Ni J, Zhang S, et al.: Accelerating Corrosion of Pure Magnesium Co-implanted with Titanium in Vivo. Sci Rep 2017;7:41924.

Tables

Table 1. Qualitative evaluation of cytotoxicity of uncoated and PLLA-coated Mg membrane in cytotoxicity test.

Well	Confluent monolayer	Cells without intracellular granulation	Reactivity[a]	Grade[a]
Uncoated Mg	(+)	0	None	0
PLLA-coated Mg	(+)	0	None	0
Media control	(+)	0	None	0
Positive control	(−)	N/A	Severe	4

PLLA, poly-L-lactic acid; Mg, magnesium; (+), positive; (−), negative; N/A, not applicable; and [a], evaluated according to reactivity grades for direct contact test of ISO 10993-5.

Figure legends and figures
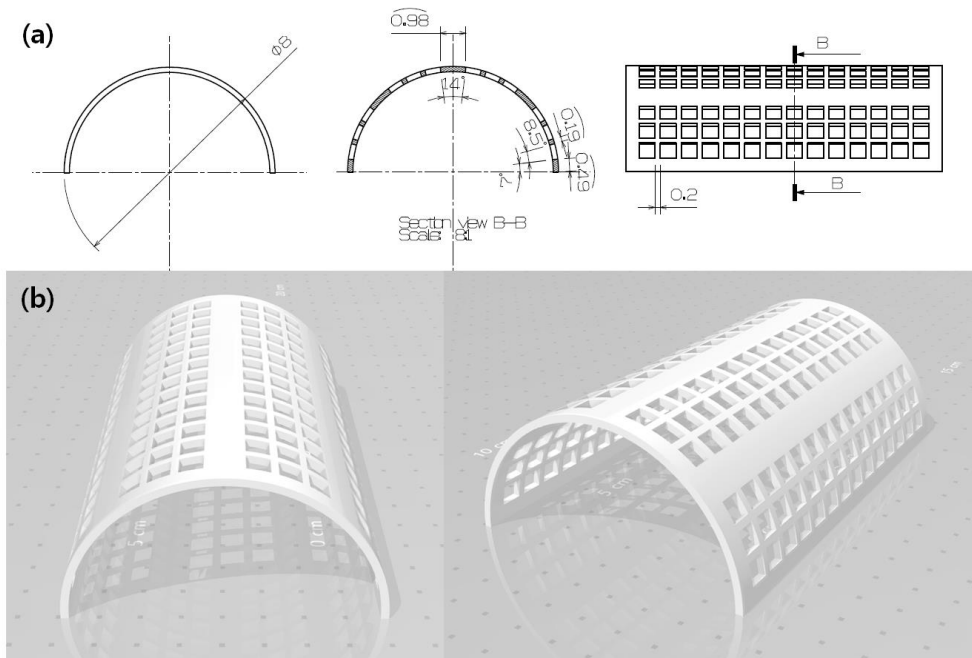
Figure 1. The design drawing (a) and three-dimensional shape (b) of the Mg membrane. All figures shown in figure (a) are in mm.
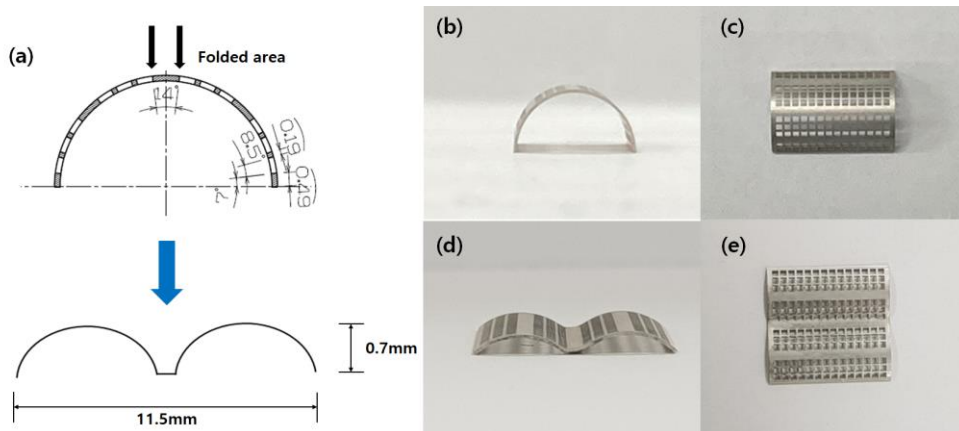
Figure 2. Schematic folding process (a) and front and top view of Mg membrane before [(b), (c)] and after [(d), (e)] folding.
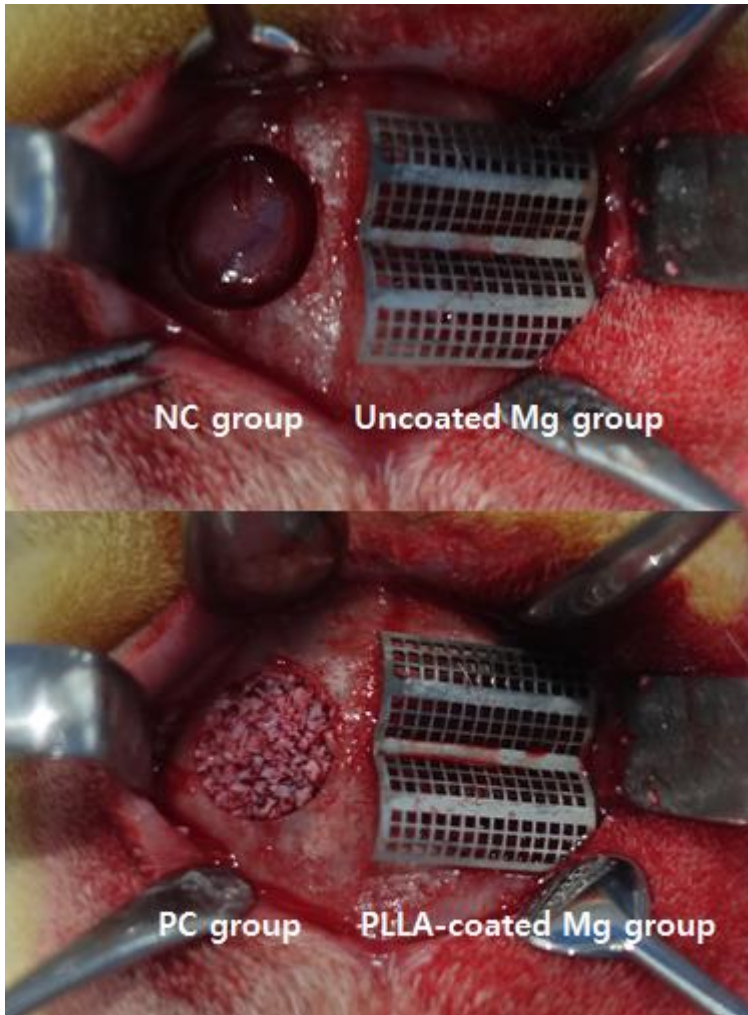
Figure 3. Clinical images showing the group assignment. Two defects per rabbit were randomly assigned to either the NC or PC group on the right side and the uncoated Mg group or the PLLA-coated Mg group on the left side, respectively.
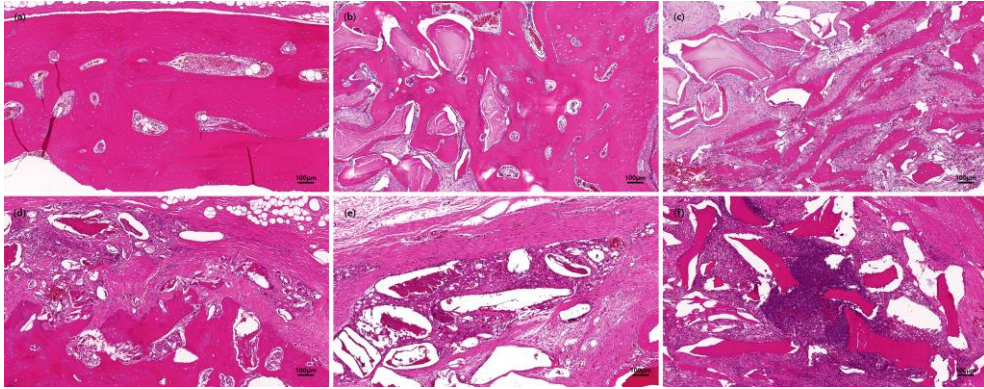
Figure 4. Representative histologic images for each scale [scale 0 (a), scale 1 (b), scale 2 (c), scale 3 (d), scale 4 (e), and scale 5 (f)] in the inflammatory response scoring system.
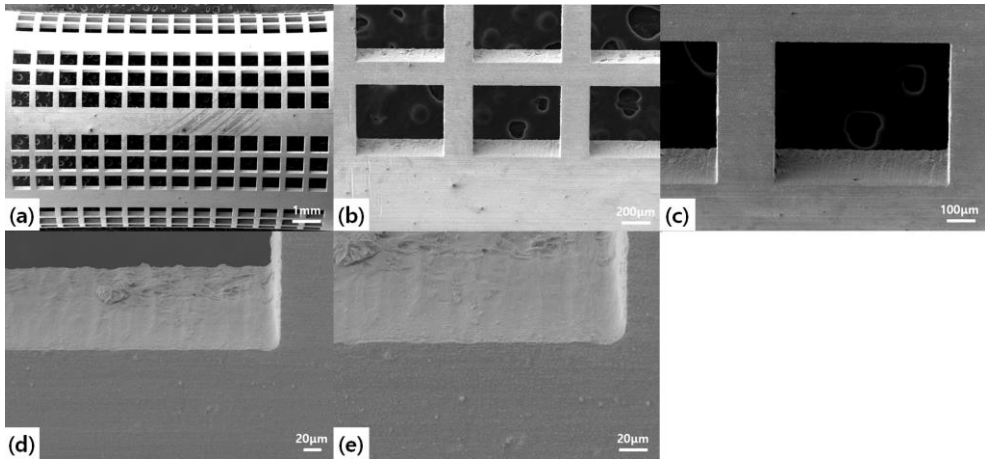
Figure 5. SEM images of the uncoated Mg membrane. Original magnification of x10 (a), x50 (b), x100 (c), x300 (d), and x500 (e).
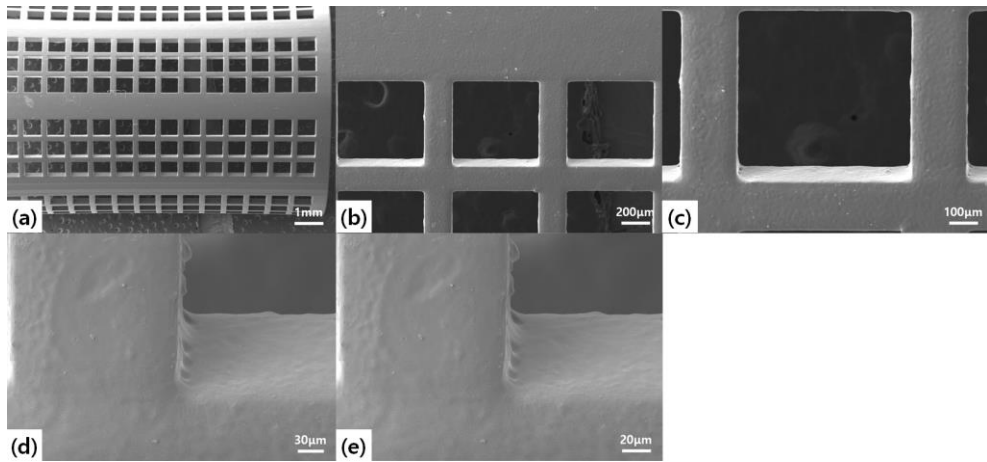
Figure 6. SEM images of the PLLA-coated Mg membrane. Original magnification of x10 (a), x50 (b), x100 (c), x300 (d), and x500 (e).
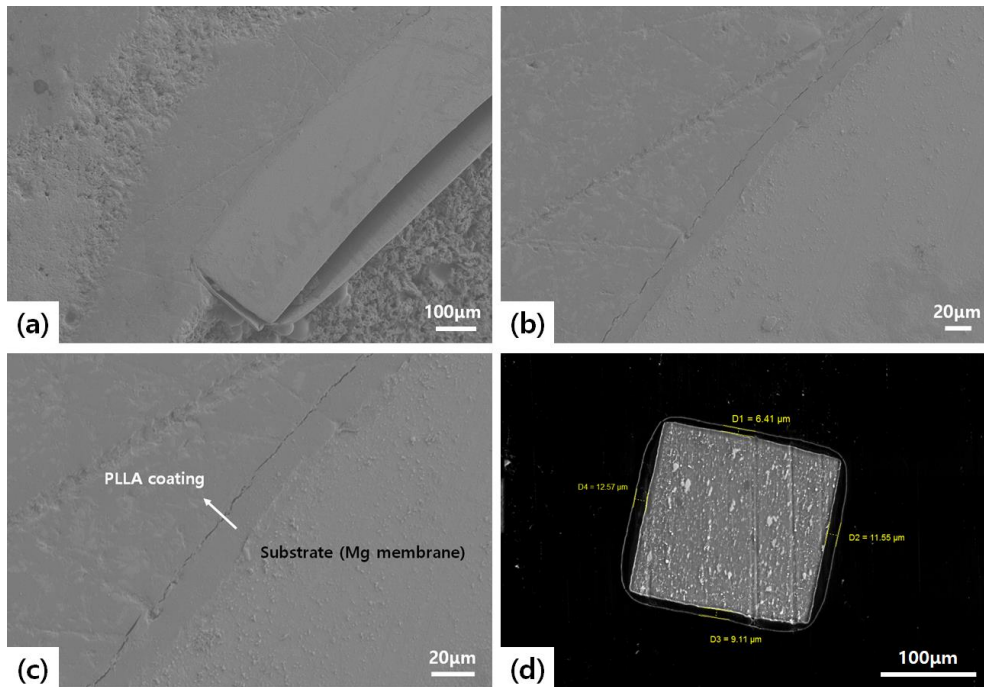
Figure 7. Microscopic images of PLLA coating [Original magnification of x100 (a), x300 (b), and x500 (c, d)] and measurement of the thickness of PLLA coating by SEM (d).
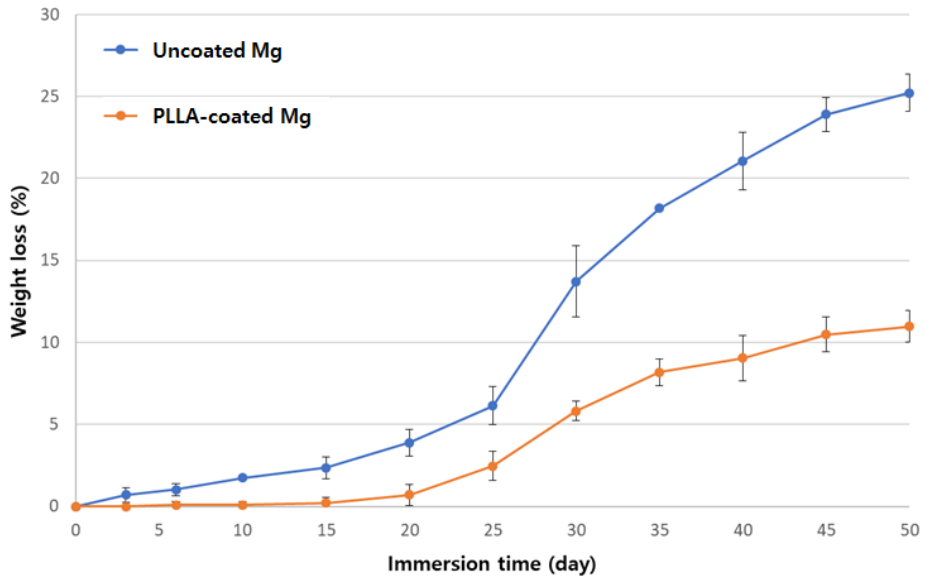
Figure 8. A line graph showing the weight changes in Mg membrane with or without PLLA coating during immersion in DMEM for 50 days.
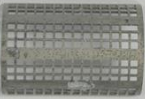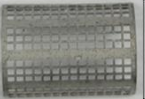
	Uncoated Mg membrane			PLLA-coated Mg membrane		
	Specimen #1	Specimen #2	Specimen #3	Specimen #1	Specimen #2	Specimen #3
5 days						
20 days						
50 days						

Figure 9. Photographic images showing the changes in the shapes of Mg membranes with or without PLLA coating during the degradation test.
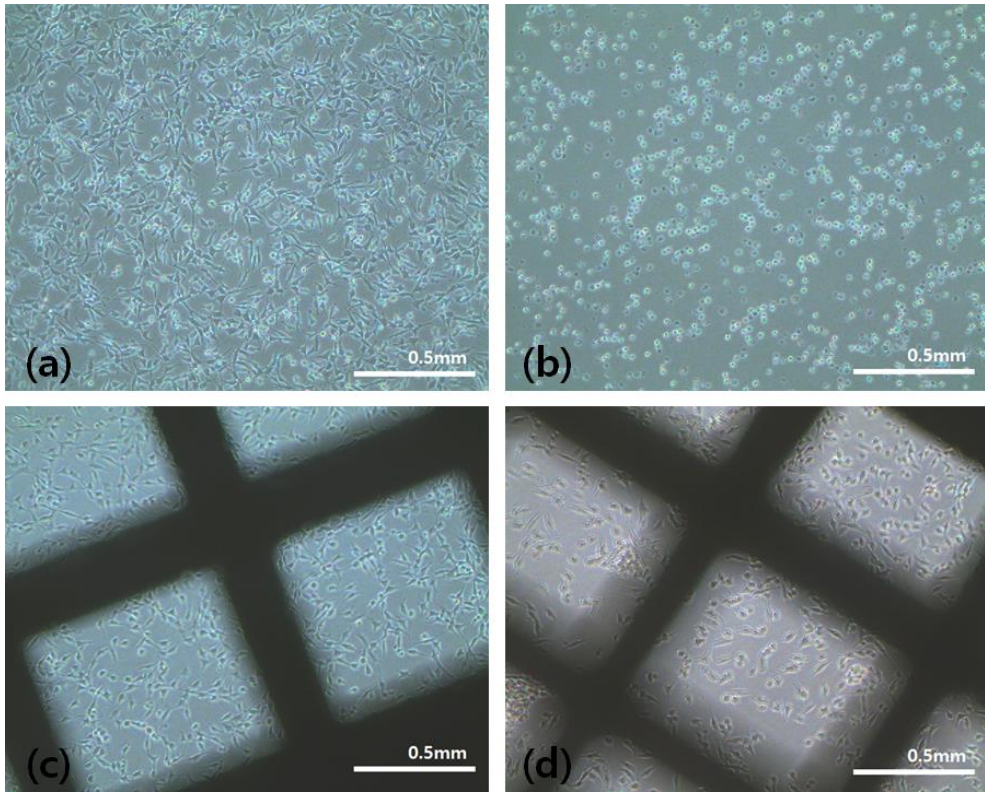
Figure 10. Microscopic observation of the growth inhibition and lysis state of L-929 cells after treatment with MC (a), PC (b), uncoated Mg membrane (c), and PLLA-coated Mg membrane (d), and culturing for 24 hours.
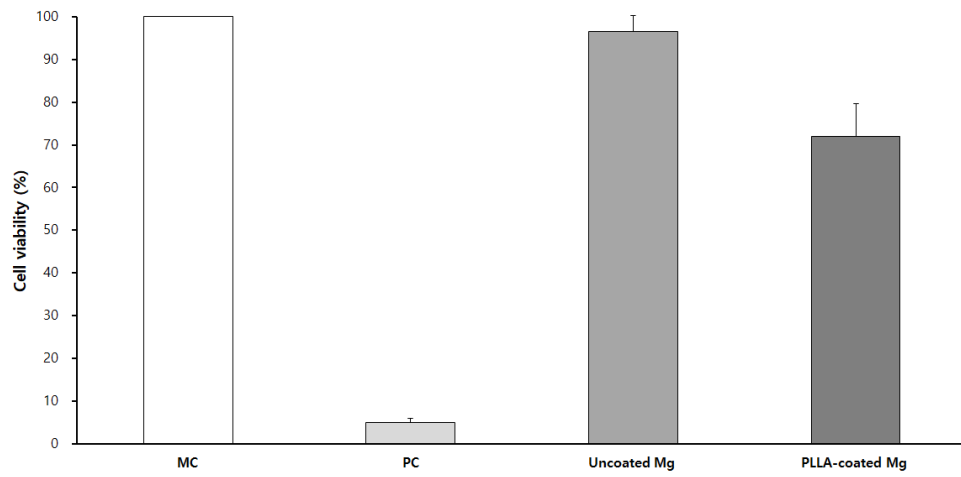
Figure 11. The results of L−929 cell viability in MTT assay.

(a)

Percentage of new bone volume

(b)

Percentage of residual material volume

(c)

Percentage of total bone volume
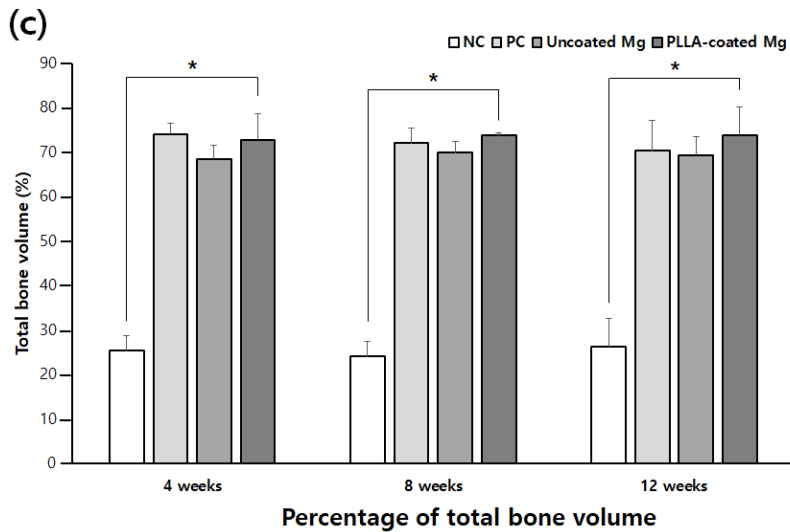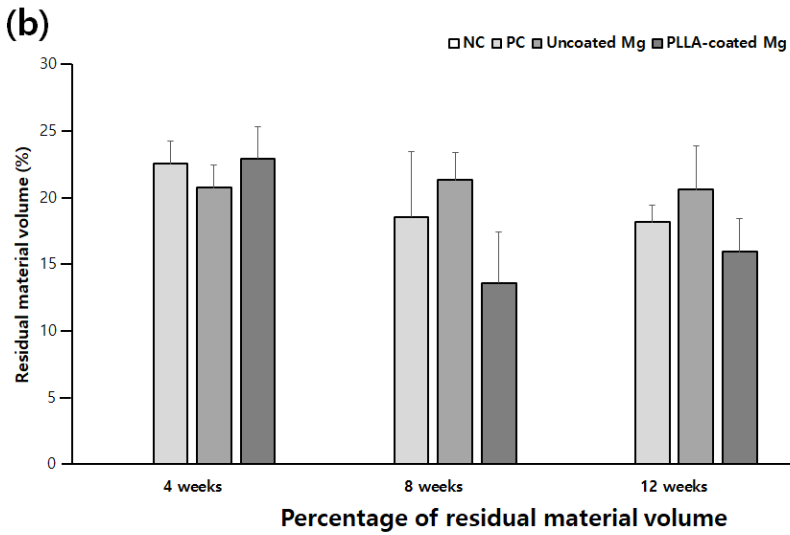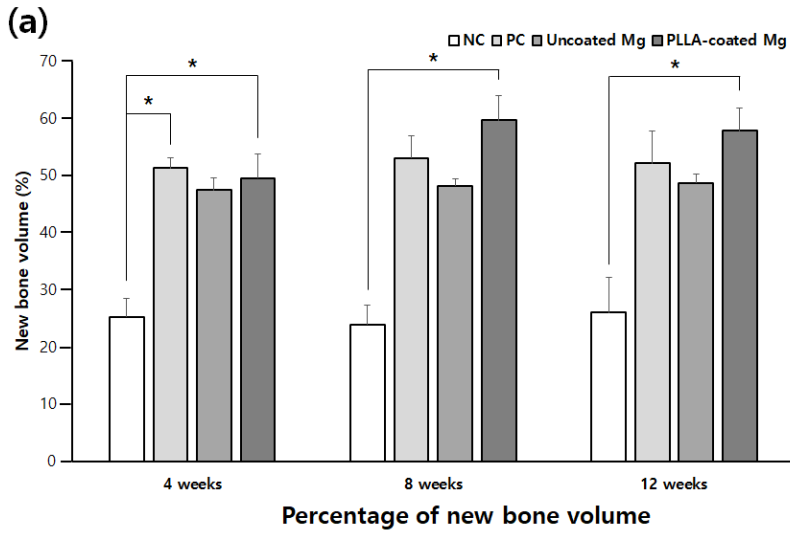
Figure 12. Comparison of percentages of NBV (a), RMV (b), and TBV (c) by quantitative analysis using micro−CT among the groups at 4, 8, and 12 weeks (* represents $P < 0.05$).
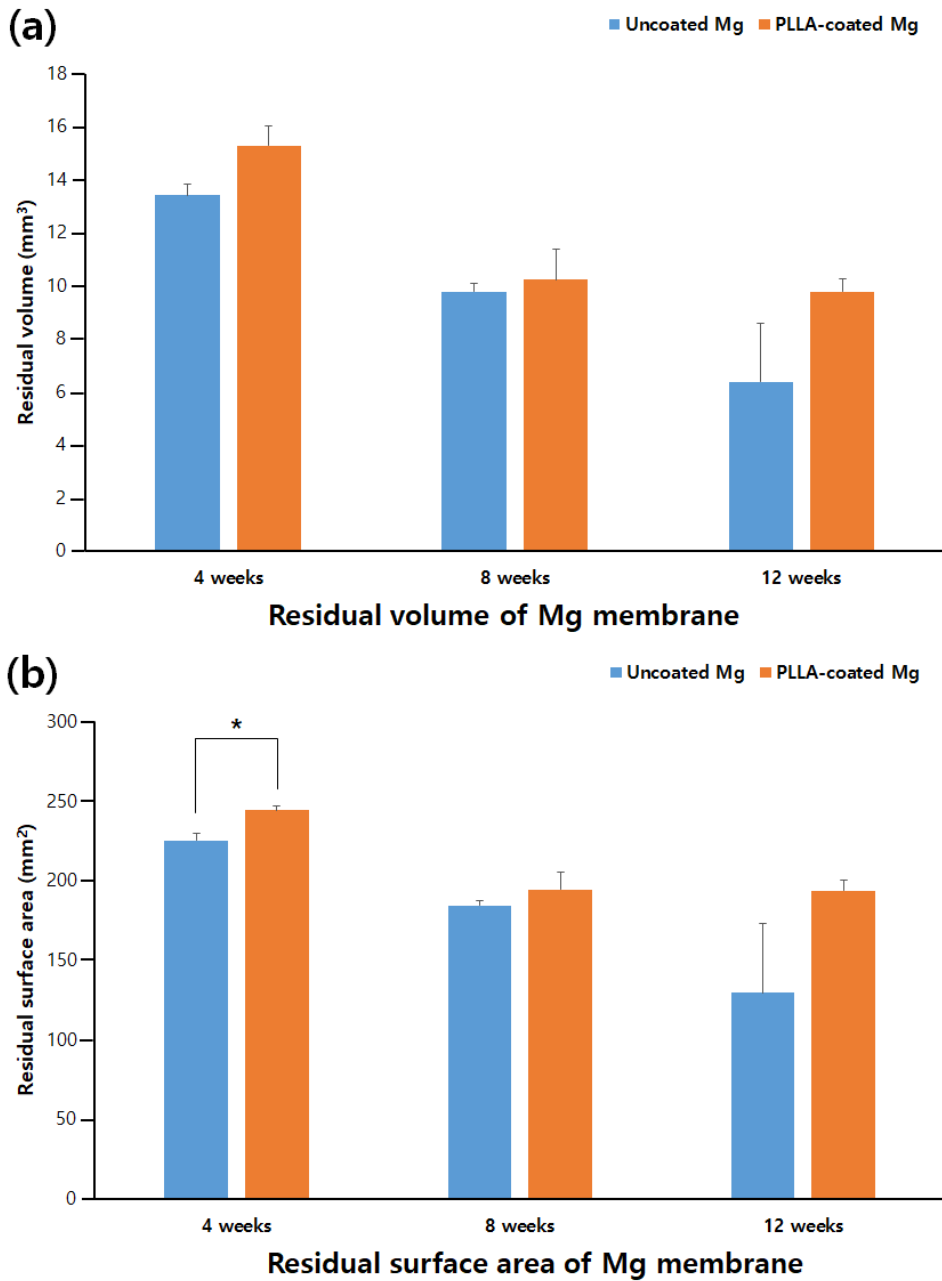
Figure 13. Comparison of residual volume (a) and surface area (b) of the Mg membrane between the uncoated Mg group and PLLA-coated Mg group (* represents $P < 0.05$).

	Uncoated Mg	**PLLA-coated Mg**
4 weeks		
8 weeks		
12 weeks		
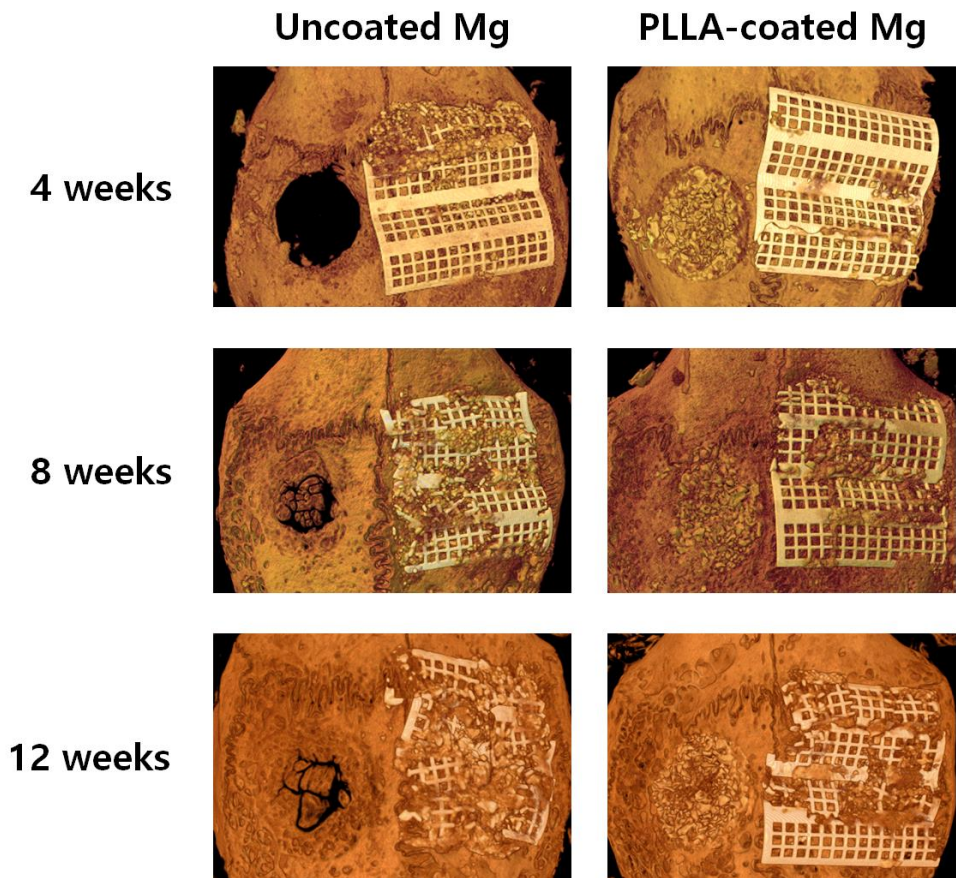
Figure 14. 3D reconstruction images showing the shape of residual Mg membrane in uncoated Mg and PLLA−coated Mg group at 4, 8, and 12 weeks.
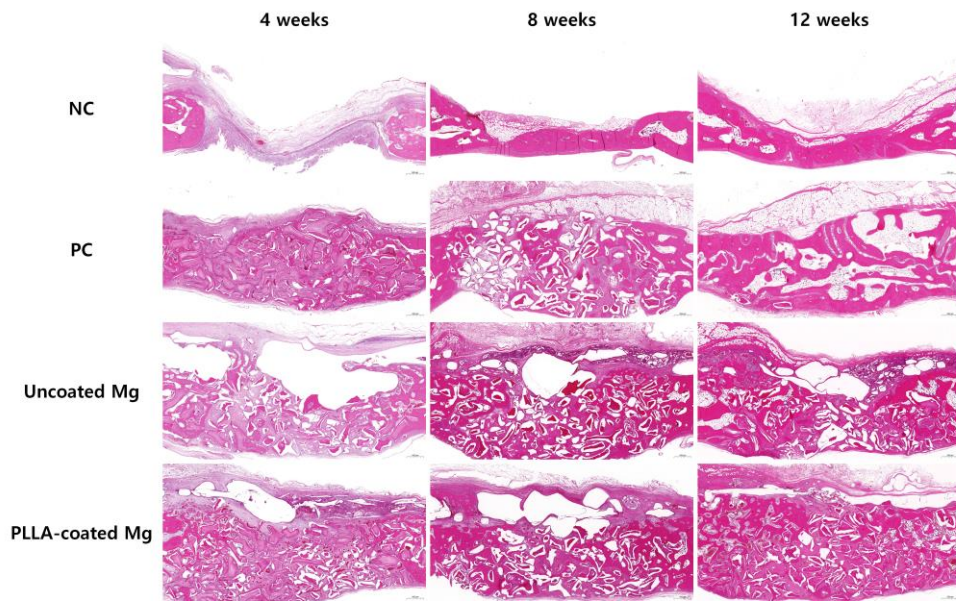
Figure 15. Representative H & E−stained histologic images for each group at 4, 8, and 12 weeks of healing period.
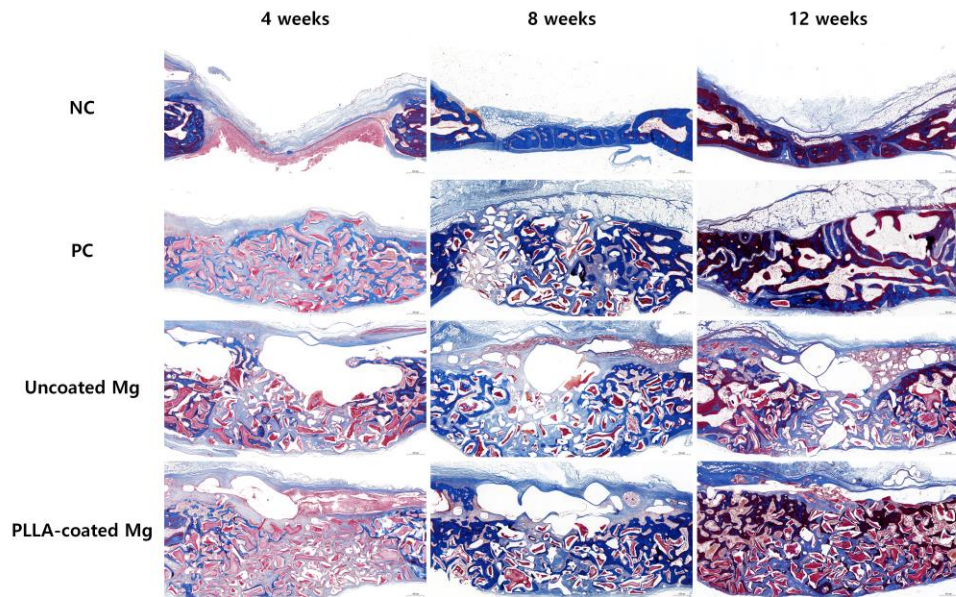
Figure 16. Representative MT–stained histologic images for each group at 4, 8, and 12 weeks of healing period.

(a)

□ NC □ PC ▨ Uncoated Mg ▨ PLLA-coated Mg

New bone area (%)

Percentage of new bone area

(b)

□ NC □ PC ▨ Uncoated Mg ▨ PLLA-coated Mg

Residual material area (%)

Percentage of residual material area

(c)

□ NC □ PC ▨ Uncoated Mg ▨ PLLA-coated Mg

Total bone area (%)

Percentage of total bone area
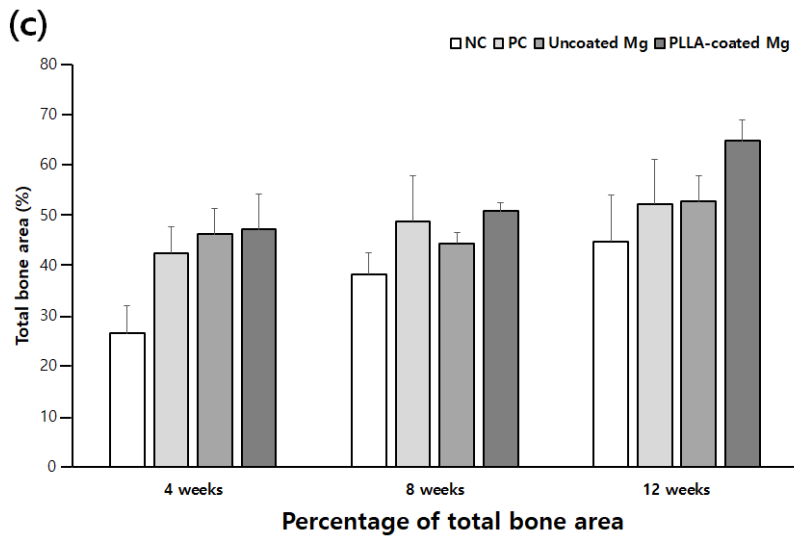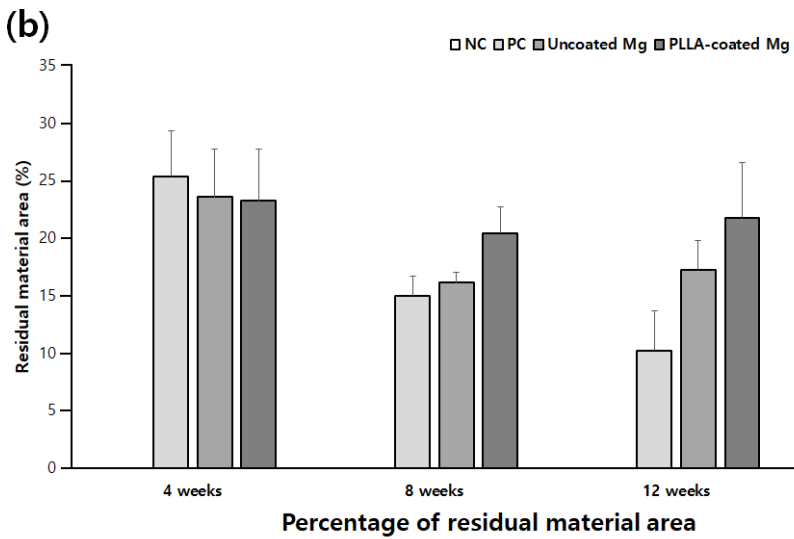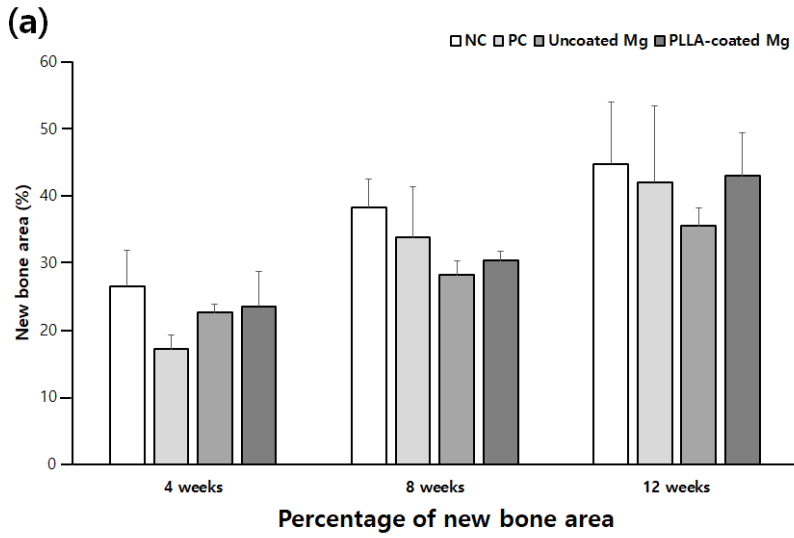
Figure 17. Comparison of percentages of NBA (a), RMA (b), and TBA (c) by histomorphometric analysis among the groups at 4, 8, and 12 weeks.
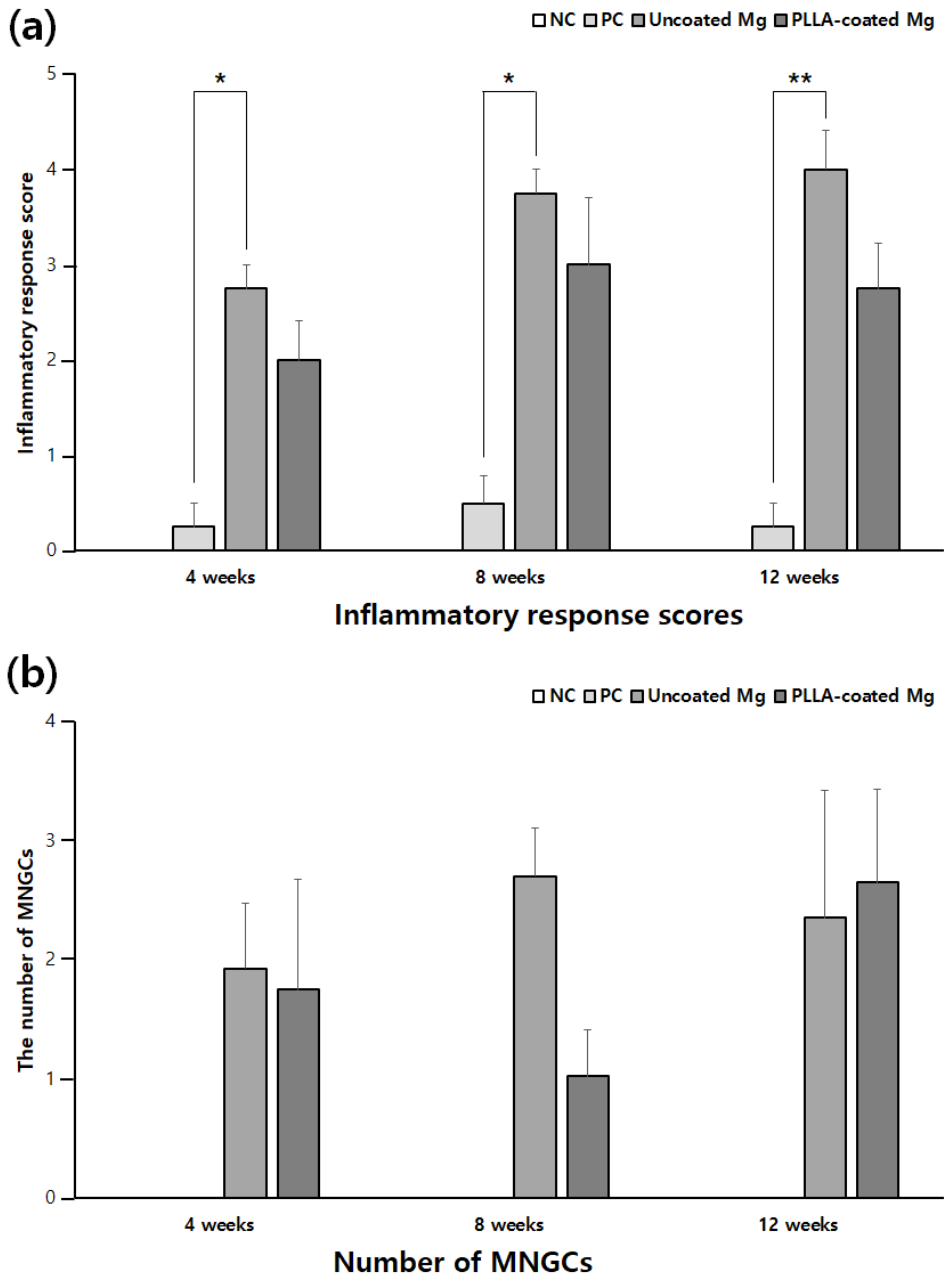
Figure 18. Comparison of inflammatory response score (a) and the number of MNGCs (b) among the groups at 4, 8, and 12 weeks (* and ** represent $P < 0.05$ and $P < 0.01$, respectively).
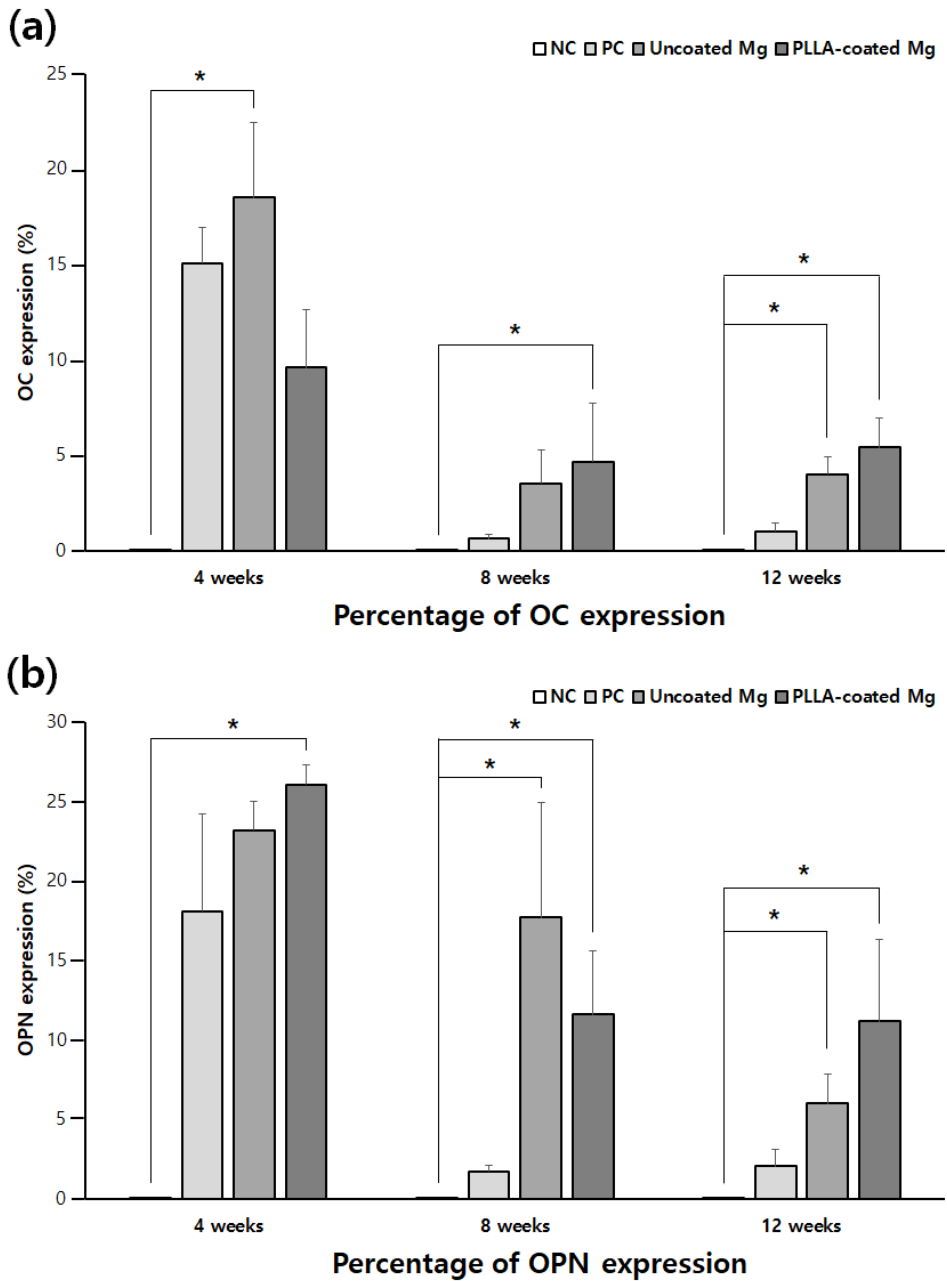
Figure 19. Comparison of percentages of OC expression (a) and OPN expression (b) by immunohistochemical analysis among the groups at 4, 8, and 12 weeks ($*$ represents $P < 0.05$).

	4 weeks	8 weeks	12 weeks
NC			
PC			
Uncoated Mg			
PLLA-coated Mg			
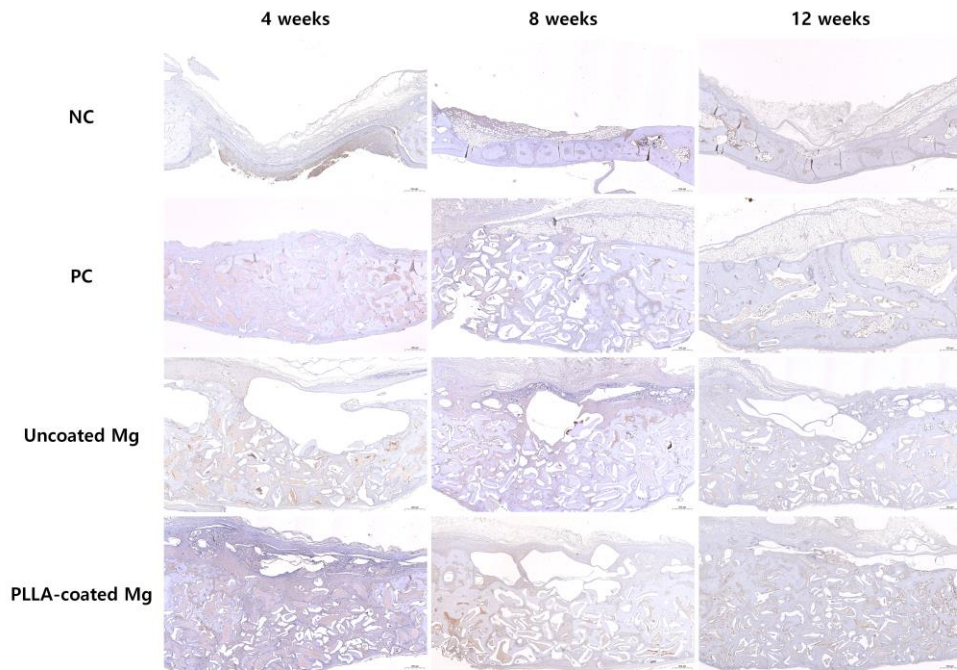
Figure 20. Representative immunohistochemical images showing OC expression for each group at 4, 8, and 12 weeks of healing period.
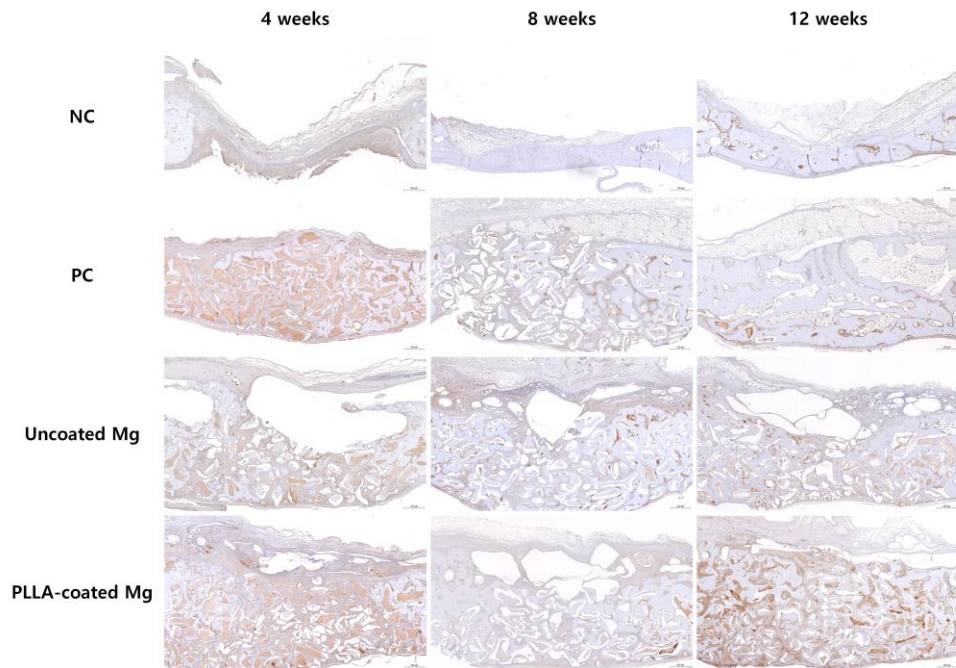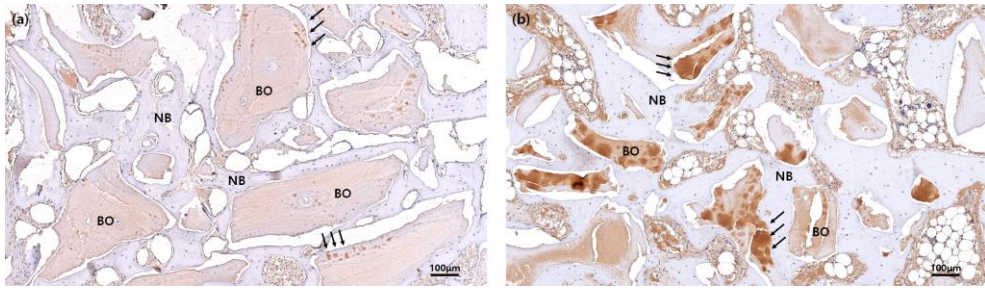
Figure 21. Representative immunohistochemical images showing OPN expression for each group at 4, 8, and 12 weeks of healing period.

Figure 22. Representative immunohistochemical images showing the major expression sites of OC (a) and OPN (b). OC and OPN showed a tendency to be expressed mainly around Bio−Oss® (arrow) (NB and BO represent new bone and Bio−Oss®, respectively).

토끼 두개골 모델에서의 중합체 코팅 마그네슘 차폐막의 골 유도 재생술에 대한 안전성 및 효용성

온 성 운

서울대학교 대학원 치의과학과 구강악안면외과학 전공

(지도교수 최 진 영)

연구 목적

임플란트 식립을 위한 골유도재생술(guide bone regeneration)은 예지성이 있는 술식이다. 공간유지 및 이식재의 안정을 위한 목적으로서, expanded polytetrafluorethylene (e-PTFE), 티타늄 강화 e-PTFE, 티타늄 mesh와 같은 비흡수성 차폐막이 사용된다. 이러한 비흡수성 차폐막은 제거를 위한 이차적인 수술이 필요하다는 큰 단점이 존재한다. 따라서 흡수성 및 비흡수성 차폐막의 장점을 가지는 새로운 차폐막의 개발에 대한 필요성이 대두되었다. 마그네슘(magnesium, Mg)은 금속의 강도를 보이면서도 생분해가 가능하다는 장점을 가지고 있다. 하지만, 생분해 시 빠른 부식이 발생하여 과도한 수소 가스의 발생과 기계적 강도의 조기 소실을 야기하게 된다. 마그네슘의 조기 부식을 막기 위하여 Poly-L-lactic acid (PLLA)와 같은 생분해 중합체를 표면처리 재료로 적용하려는 시도들이 있어왔다. 하지만 대부분 *in vitro* 수준의 연구들이며 *in vivo* 연구는 부족한 실정이다. 따라서 PLLA 코팅 마그네슘 합금의 개선된 부식 저항성 및 안전성과 효용성에 대한 더 많은 *in vivo* 연구가 필요한 상황이다. 본 연구의 목적은 *in vitro* 시험 및 토끼 두개골

모델을 이용한 *in vivo* 시험을 통하여 PLLA 코팅 마그네슘 차폐막의 골유도재생술에 대한 안전성 및 효용성을 평가하는 것이었다.

재료 및 방법

마그네슘-디스프로슘(dysprosium) 합금을 사용하여 코팅되지 않은 마그네슘 차폐막 및 PLLA로 코팅된 마그네슘 차폐막이 제작되었다. 주사전자현미경(scanning electron microscope, SEM)을 사용하여 비코팅 및 PLLA 코팅 마그네슘 차폐막의 표면에 대한 미세구조가 관찰되었고, PLLA 코팅의 두께 측정이 시행되었다. Dulbecco's modified Eagle medium (DMEM)에 마그네슘 차폐막을 담그고 시간에 따른 무게 감소를 측정함으로써 *in vitro* 분해시험을 수행하였다. ISO 10993-5에 따라 *in vitro* 세포독성시험이 시행되었고, 3-(4,5-dimethylthiazol-2-yl)-2,5-diphenyltetrazolium bromide (MTT) 분석(assay)이 수행되었다. *In vivo* 시험이 24마리의 건강한 뉴질랜드 토끼를 이용하여 진행되었다. 두개골의 양측에 대칭적인 8 mm 직경의 2개의 골 결손부를 트레핀버를 이용하여 형성하였다. 총 48개의 결손부 중 12개의 결손부가 다음 4개의 군에 무작위로 배정되었다: (1) 음성 대조군(NC 군): 골이식재로 채우지 않고 차폐막을 적용하지 않음, (2) 양성 대조군(PC 군): 골이식재로 채우고 차폐막을 적용하지 않음, (3) 비코팅 마그네슘 군(비코팅 Mg 군): 골이식재로 채우고 비코팅 마그네슘 차폐막을 적용, (4) PLLA 코팅 마그네슘 군(PLLA-코팅 Mg 군): 골이식재로 채우고 PLLA 코팅 마그네슘 차폐막을 적용. 결손부를 채우기 위한 골이식재로서 이종골이식재(Bio-Oss®; Geistlich Pharma AG, Wolhusen, Switzerland)가 사용되었다. 임상 관찰이 정기적으로 시행되었고, 8마리의 토끼(16개의 결손부)가 각 실험시기별 치유 양상을 분석하기 위해 4주, 8주, 12주로 나누어 희생되었다. Micro-computed tomography (micro-CT)를 이용한 방사선학적 분석 및 조직학적, 조직계측학적, 면역조직화학적 분석이 각 표본에 시행되었다. 각 실험시기별 군 간의 변수 차이를 비교하기 위해 통계학적 분석이 수행되었고 0.05 미만의 *P* 값을 통계학적으로 유의하

다고 간주하였다.

연구 결과

 PLLA 코팅 마그네슘 차폐막은 코팅되지 않은 마그네슘 차폐막에 비해 전반적으로 부드러운 표면 형태를 보였고, PLLA 코팅의 두께는 SEM에 의해 9.91 ± 2.75 μm로 측정되었다. 비코팅 및 PLLA 코팅 마그네슘 차폐막의 분해 정도를 관찰한 결과는 PLLA 코팅의 양호한 보호 효과를 시사하였다. 세포독성시험에서 ISO 10993-5의 추출물 세포독성에 대한 정성적 형태학적 등급화에 근거하였을 때, 비코팅 및 PLLA 코팅 차폐막의 표본 하에서 변형되거나 변성된 세포들은 관찰되지 않았다. MTT 분석에서의 L-929 cell viability의 결과는 비코팅 마그네슘 차폐막의 경우 96.5%의 cell viability를 보인 반면, PLLA 코팅 마그네슘 차폐막은 그보다 다소 낮은 72%의 cell viability를 보였다. 하지만 ISO 10993-5의 MTT 세포독성시험의 평가 기준에 근거하였을 때, 두 차폐막 모두 세포독성 잠재성이 없는 것으로 확인되었다. *In vivo* 실험에 있어서 실험 기간 동안 사망한 토끼는 없었고, 한 마리를 제외한 모든 토끼가 임상 관찰상 창상 열개, 차폐막 노출, 부종, 누공 형성과 같은 합병증없이 치유되었다. Micro-CT를 이용한 방사선학적 분석에서 PLLA-코팅 Mg 군은 4주, 8주, 12주에서 NC 군에 비해 유의하게 높은 신생골부피백분율 및 총골부피백분율을 보였다 (모두 $P < 0.05$). PLLA-코팅 Mg 군의 잔존차폐막 표면적은 4주에서 비코팅 Mg 군에 비해 유의하게 높았다 ($P < 0.05$). 조직학적 관찰 시, PLLA-코팅 Mg 군은 차폐막 하방에 큰 공극 부위를 형성하였으나, 비코팅 Mg 군에 비해 더 작고 더 늦게 관찰되었다. 또한 PLLA-코팅 Mg 군은 비코팅 Mg 군에 비해 골 형태의 더 완전한 회복을 보였다. 조직형태계측 분석에서 PLLA-코팅 Mg 군은 모든 연구 시기에서 가장 높은 총골영역백분율을 보였고, 8주와 12주에서 가장 높은 잔존이식재영역백분율을 보였으나, 통계학적으로 유의하지는 않았다. 각 군간의 염증반응점수 및 다형핵거대세포의 개수를 비교한 결과, PLLA-코팅 Mg 군은 염증반응점수 및 다형핵거대세포의 개수에 있

어서 음성 및 양성 대조군과 유의한 차이를 보이지 않았다. Osteocalcin (OC) 및 osteopontin (OPN)을 이용한 면역조직화학적 분석에서 PLLA-코팅 Mg 군의 8주에서 OC발현백분율은 NC 군에 비해 유의하게 높았고 ($P < 0.05$), OPN발현백분율은 NC 군에 비해 4주, 8주, 12주에서 유의하게 높았다 (모두 $P < 0.05$).

결론

 PLLA 코팅 마그네슘 차폐막의 안전성에 있어서, PLLA 코팅 마그네슘 차폐막은 세포독성시험에서 세포독성효과를 보이지 않았고, 토끼 두개골 모델을 통한 *in vivo* 실험에서 조직학적 및 임상적으로 유의한 염증반응을 보이지 않았기 때문에 양호한 생적합성을 보여주었다. 효용성의 측면에서, 분해검사와 Micro-CT 분석상 PLLA 코팅 마그네슘 차폐막은 비코팅 마그네슘 차폐막에 비해 늦은 분해 양상을 보였다. 또한 방사선학적 및 조직형태계측학적 분석에서 우수한 골형성 및 유지 능력을 보였다. 본 연구의 결과를 통해 PLLA 코팅 마그네슘 차폐막은 *in vitro* 및 *in vivo* 수준에서 골유도재생술을 위한 안전하고 효과적인 재료로 사료된다.

감사의 글